

MINISTRY OF EDUCATION AND SCIENCE OF UKRAINE  
KYIV NATIONAL UNIVERSITY OF TECHNOLOGIES AND DESIGN

Faculty of Chemical and Biopharmaceutical Technologies  
Department of Industrial Pharmacy

*Master's thesis*

on the topic RESEARCH OF DEGRADATION OF ANTIBIOTICS BY ADVANCED OXIDATION  
TECHNOLOGY BASED ON SULFATE RADICALS

Completed: student of the group MPhch-20  
of the specialty 226 Pharmacy, industrial pharmacy  
(code and title of the specialty)

Zhao GUANGLI  
(first name, last name)

Supervisor \_\_\_\_\_ Andrii HALSTIAN  
(first name, last name)

Reviewer \_\_\_\_\_ Anna KHARYTONENKO  
(first name, last name)

KYIV NATIONAL UNIVERSITY OF TECHNOLOGIES AND DESIGN

Institute, faculty Chemical and Biopharmaceutical Technologies  
 Department Industrial Pharmacy  
 Speciality 226 Pharmacy, industrial pharmacy  
 (code and title)

**Approve**  
 Head of Department Industrial Pharmacy,  
 Professor, Doctor of Pharmaceutical Science  
 Vladyslav STRASHNYI

\_\_\_\_\_  
 "14" December 2021

## ASSIGNMENTS FOR THE MASTER'S THESIS

Zhao Guangli

\_\_\_\_\_  
 (Full Name)

1. Thesis topic Research of degradation of antibiotics by advanced oxidation technology based on sulfate radicals

2. Scientific supervisor Andrii Halstian, Professor, Doctor of Science  
 (first name, last name, patronymic, academic degree, academic title)

Approved by the order of the higher education al institution on 4thOctober 2021, N286

3. Dead line for student submission of work 14th December 2021

4. Initial data for work: scientific and information sources, methodological and technological literature, scientific periodicals, international and domestic regulations and standards for the development and production of medicines

5. Content of the thesis (list of questions to be developed).*In accordance to the content and task to work(For example: a review of the literature on antibacterial hydrogels, the development of methods for the manufacture of antibacterial hydrogels, the study of the properties of antibacterial hydrogels ..).*

\_\_\_\_\_  
 \_\_\_\_\_  
 \_\_\_\_\_  
 \_\_\_\_\_

6. Consultants of the master's thesis sections

Section	Surname, initials and position of the consultant	Signature	
		The task was issued	the task accepted
Section 1	Andrii Halstian, Professor, PhD		
Section 2	Andrii Halstian, Professor, PhD		
Section 3	Jianjun Song, Professor, PhD	宋建军	
Section 4	Jianjun Song, Professor, PhD	宋建军	

7. Date of issue of the assignment September 20, 2021

**Execution schedule**

No	The name of the stages of the master's thesis	Terms of performance of stages	Note on performance
1	Introduction	20.09 – 27.09.2021	赵广立
2	Section1 Analysis of literature sources	28.09. – 11.10.2021	赵广立
3	Section2 Material and methods	12.10 – 25.10.2021	赵广立
4	Section3 Characterization and catalytic performance of MOFs derived CoMn-LDH and CoFe-LDH	26.10 – 01.11.2021	赵广立
5	Section 4 Catalytic performance of cobalt based Alumina pellets	02.11 – 08.11.2021	赵广立
6	Conclusions	09.11.-15.11.2021	赵广立
7	Draw up a master's thesis( <i>final version</i> )	16.11.-04.12.2021	赵广立
8	Submission of master's thesis to the department for review ( <i>14 days before the defence</i> )	06.12.-14.12.2021	赵广立
9	Checking the master's thesis for signs of plagiarism( <i>10 days before the defence</i> )	14.12-18.12.2021	赵广立
10	Submission of master's thesis to the master's department to check the implementation of supplement to the individual curriculum ( <i>10 days before the defence</i> )	16.12-18.12.2021	赵广立
11	Submission of master's thesis for approval by the head of the department( <i>from 7 days before the defence</i> )	18.12-21.12.2021	赵广立

Student \_\_\_\_\_  
(signature)

赵广立

Zhao GUANGLI  
(first name, last name)

Scientific supervisor \_\_\_\_\_  
(signature)

Andrii HALSTIAN  
(first name, last names)

Head of the scientific and methodological center  
for the management of specialist training  
(signature)

Olena HRYHOREVSKA  
(first name and second name)

## SUMMARY

**Zhao Guangli. Research of degradation of antibiotics by advanced oxidation technology based on sulfate radicals. – Manuscript.**

With the continuous progress of science and technology, environmental protection has become an important issue of social sustainable development. Among them, the problem of water resources protection is particularly prominent. Among the many factors causing water pollution, the wanton discharge of domestic sewage and industrial and pharmaceutical wastewater has become one of the main pollution sources, especially the pollution of a large number of high concentration wastewater containing antibiotics and anti-inflammatory. When these antibiotics and anti-inflammatory organics reach a certain concentration in the environment and wastewater, they will seriously threaten the environment of ecology and human survival. In recent years, the treatment of these antibiotic wastewater has become the focus and research field of many scholars. Advanced oxidation technology based on sulfate radical ( $\text{SO}_4^{\bullet-}$ ) has attracted extensive attention of researchers because of its high efficiency and strong applicability. It is an effective method to treat antibiotic wastewater. The technology of producing  $\text{SO}_4^{\bullet-}$  with persulfate (PMS) as oxidant is a research hotspot at present. Existing studies have found that although the activation of PMS with cobalt ions to produce  $\text{SO}_4^{\bullet-}$  is efficient, there is secondary pollution of cobalt. Although the traditional cobalt based oxide catalyst controls the secondary pollution of cobalt ions to a certain extent, the reaction rate is low. Therefore, the study of new high-efficiency catalysts is of great significance.

In this paper, MOFs was selected as the precursor and LDH with high specific

surface area was prepared by alkaline etching. It showed high activity in the degradation of tetracycline hydrochloride activated by PMS. Since the LDH catalyst derived from MOFs is also in powder state, the catalyst needs to be separated by filtration or centrifugation after pollutant degradation, which increases the operation cost. To solve this problem, we loaded the active component cobalt on the alumina ball, so as to solve the problem of difficult separation of the catalyst.

*Keywords: antibiotics; PMS; MOFs; Tetracycline hydrochloride; alumina*

## АНОТАЦІЯ

**Чжао Гуанлі. Дослідження деградації антибіотиків передовою технологією окислення на основі сульфатних радикалів. – Рукопис.**

З безперервним прогресом науки і техніки охорона навколишнього середовища стала важливою проблемою соціального сталого розвитку, особливо помітною є проблема охорони водних ресурсів. Серед багатьох факторів, що спричиняють забруднення води це скид побутових і промислових стічних вод. В останні роки очищення стічних вод від антибіотиків стало вагомим сферою досліджень багатьох вчених. Технологія окислення на основі сульфатного радикала ( $\text{SO}_4^{\bullet-}$ ) привертає увагу дослідників завдяки своїй високій ефективності та широкому застосуванню. Одержання  $\text{SO}_4^{\bullet-}$  з персульфату (ПМС) є зараз гарячою точкою досліджень. Вони показали, що хоча активація ПМС іонами кобальту для утворення  $\text{SO}_4^{\bullet-}$  ефективна, є вторинне забруднення кобальтом. Тому вивчення нових високоефективних каталізаторів має велике значення.

У цій роботі було обрано каталізатори з високою питомою поверхнею. Вони показали високу активність у деградації гідрохлориду тетрацикліну. Оскільки каталізатор LDH, отриманий з MOF, також знаходиться в порошковому стані, його необхідно відокремити фільтрацією або центрифугуванням після деградації забруднюючої речовини, що збільшує вартість експлуатації. Щоб вирішити цю проблему було завантажено активний компонент кобальт на кульку глинозему.

*Ключові слова:* антибіотики; персульфат, тетрацикліну гідрохлорид; глинозем.

## Content

Introduction.....	8
Chapter 1. Analysis of literature sources.....	11
1.1 Treatment method of antibiotic wastewater.....	11
1.2 Overview of peroxide advanced oxidation system.....	26
1.3 Advanced oxidation technology based on persulfate.....	31
1.4 Co/PMS catalytic oxidation system.....	35
1.5 Research ideas.....	43
Chapter 2. Material and methods.....	45
2.1 Chemical reagents.....	45
2.2 Synthesis of MOFs-derived LDH catalysts.....	45
2.3 Synthesis of cobalt based Alumina pellets.....	46
2.4 Characterization.....	46
2.5 Catalytic degradation experiments.....	47
2.6 Phytotoxicity assessment.....	48
Chapter 3. Characterization and catalytic performance of MOFs derived CoMn-LDH and CoFe-LDH.....	50
3.1 Characterization of MOFs-derived LDH catalysts.....	50
3.2 Catalytic performance.....	55
3.3. Influence of 2, 4-DCP degradation parameters.....	58
3.4 Degradation test of multiple pollutants.....	59
3.5 Stability and reusability of LDHs.....	61
3.6 Identification of reaction species and possible mechanism.....	62

3.7 Phytotoxicity assessment.....	66
3.8 Conclusion.....	69
Chapter 4. Catalytic performance of cobalt based Alumina pellets.....	71
4.1 Results and discussion.....	73
4.2 Conclusion.....	77
Conclusion and research prospect.....	78
5.1 Conclusions.....	78
5.2 Research prospect.....	79
Reference.....	80

## **Introduction**

With the rapid development of industrialization, the economy is also developing rapidly. People not only enjoy the convenience brought by these developments, but also bring a lot of damage and pollution to the surrounding environment. Problems such as energy shortage and environmental pollution limit human survival and development, and become an important problem to be solve durgently. Water is an indispensable precious resource for human survival and development, but in recent years, water resource crisis has become one of the most serious problems facing mankind. Some polluted water bodies contain a large number of heavy metals and refractory organic pollutants, such as antibiotics, heavy metals and environmental hormones. These pollutants will enter the human body or animals through the food chain or direct contact, affect the synthesis, metabolism and endocrine processes of hormones in human or other organisms, and eventually destroy the coordination and stability of the internal environment. In addition, these pollutants will damage the human body through physical and chemical effects, resulting in teratogenicity, mutagenicity and even cancer. Therefore, how to effectively remove these pollutants is a very arduous task for water treatment.

Antibiotics refer to a class of substances with anti pathogen or other activities synthesized by microorganisms (molds, bacteria or other microorganisms) in the process of life, which can interfere with and inhibit the activity of pathogenic microorganisms to a certain extent. According to different chemical structures, antibiotics are mainly divided into macrolides, tetracyclines, sulfonamides, quinolones and antibiotics  $\beta$ - Lactams. Antibiotics, as a kind of compounds that can

effectively inhibit microbial activity, are often used to prevent and treat diseases caused by microbial infection in human medicine, animal husbandry and aquaculture. However, the overuse of antibiotics makes it exist in a large number in the water environment, induces the emergence of drug-resistant pathogens, forms a vicious circle, and causes serious harm to human and aquatic organisms. In 1928, the British scientist Fleming first extracted penicillin from the culture of *Staphylococcus aureus* contaminated by *Penicillium*. More than ten years later, penicillin was first used in clinical treatment. After continuous development, the types of antibiotics have gradually increased, up to more than 4000, but only more than 100 can be used in the medical field. Research shows that about 50% of the antibiotics produced worldwide are used in animals and animal husbandry. According to the food and drug administration, about 80% of antibiotics in the United States were used in animal husbandry in 2017. In Australia, only about 3600 tons of antibiotics are used in human society every year, while about 8000 tons of antibiotics are used in animals.

With the excessive use of antibiotics, antibiotics have been detected in many surface water basins in major countries in the world, and the content of residual antibiotics in water and soil has gradually increased, resulting in the inability of natural restoration of the ecological environment. Because of its antibacterial effect and its own group structure, antibiotics inhibit or even poison the growth and reproduction of microorganisms, animals and plants. In particular, antibiotics discharged into the water body will exist stably in the water body, which is difficult to be degraded and removed by microorganisms, resulting in bacteria producing drug-resistant genes, enhancing the drug resistance of pathogenic bacteria, and

making antibiotics ineffective in the process of disease treatment. Antibiotics in water can also inhibit microbial reproduction and normal activity, so as to change the community structure of microorganisms. It is reported that bacteria resistant to single or multiple antibiotics have been found in the sewage treated by the sewage treatment plant. These bacteria are dangerous to human life and health through the food chain through agricultural irrigation and other means; at the same time, the excessive use of antibiotics in livestock and poultry breeding industry leads to the decline of livestock and poultry immunity, the increase of mortality and the generation of secondary pollution. Due to the emergence of drug resistance, old drugs are difficult to meet the needs of clinical treatment. New drugs need to be developed continuously for treatment, resulting in a waste of resources and a threat to human life and health. Most importantly, antibiotic waste will also penetrate into the soil through the earth's large cycle, and then enter the human body through the food chain cycle, endangering health.

At present, the sources of antibiotics in water environment are mainly divided into the following ways: effluent from sewage treatment plant, pharmaceutical wastewater and solid waste, drugs for agricultural production, the use of personal care products and drugs for livestock and poultry breeding. Antibiotics are transferred to the water environment through these ways. With the accumulation of time, the content and types of antibiotics in the water environment are increasing. At present, antibiotics used in various fields can be divided into:  $\beta$ -Lactams, aminoglycosides, macrolides, tetracyclines, lincomycin, polypeptides, quinolones, sulfonamides and other antibiotics; According to the use, it can be divided into anti-bacterial antibiotics, anti

fungals antibiotics, anti-tumor antibiotics, anti-virus antibiotics, livestock antibiotics, agricultural antibiotics and other microbial drugs.

**Objective of the study:** an improved oxidation process based on a sulfate radical and the creation of efficient and inexpensive catalysts with high activity, high stability and easy separation for advanced oxidation technologies.

**The object of research** is a catalyst for the process of wastewater treatment with antibiotics.

**The subject of research** is the development and synthesis of catalysts for oxidation.

**Research methods** include catalyst preparation methods (hydrothermal method, etching method, equal volume impregnation method, etc.), catalyst evaluation methods, contaminant analysis methods and various characterization methods (XRD, SEM, EPR, XPS, etc.)

**Practical value:** This technology provides an efficient and inexpensive way to treat wastewater with antibiotics.

**Scientific novelty:** This study developed a new high surface area LDH catalyst that can effectively activate PMS and be used to degrade antibiotics. At the same time, alumina granules are used as a carrier to support the active component, which solves the problem of complex separation of powder catalyst and promotes the industrialization of advanced oxidation technologies based on activated persulfate.

## **Chapter 1 Analysis of literature sources**

### **1.1 treatment method of antibiotic wastewater**

With the deepening of people's attention to antibiotic pollution in water, researchers' research on improving existing and exploring new antibiotic wastewater treatment technologies is also greatly increasing[1-3]. At present, the methods of removing antibiotics from water are divided into three categories: biological method, physical method and chemical treatment method. Biological treatment mainly depends on the metabolic function of microorganisms in water to decompose and transform antibiotic pollutants. However, antibiotic wastewater has complex components, high concentration of organic pollutants and biological toxicity. Therefore, it is difficult to effectively degrade antibiotic pollutants in water by using a single biological treatment technology. Pretreatment is often required and combined with other treatment technologies, which inevitably prolongs the treatment cycle and increases the treatment cost.

#### **1.1.1 Physical method**

Membrane separation and adsorption are physical treatment methods commonly used to remove antibiotics. Previous studies have proved that the use of low pore size membranes in membrane treatment technologies such as nanofiltration[4, 5] and reverse osmosis[6, 7] can effectively remove antibiotics from water. It is worth noting that these membrane separation processes only change the existing state of antibiotics, do not destroy the chemical structure of antibiotics, the mineralization rate is very low and easy to flow into the environment again. In order to improve the

removal rate of small molecule antibiotics, it is often necessary to continuously reduce the pore size of the membrane, which is easy to cause membrane blockage and energy loss. The adsorption method [8, 9] is to use the strong adsorption of adsorbent to adsorb antibiotics in water and fix them, so as to reduce or inhibit the activity and harm of antibiotics. The commonly used adsorbents are solid adsorbents such as activated carbon [10, 11] and metal oxides with multi-stage pores. Among them, activated carbon has porous structure and large specific surface area, so it shows good adsorption performance. With the increase of treatment time, after the adsorbent is over saturated, it needs to be separated from the water body through solid-liquid separation technology to avoid secondary pollution. The chemical structure of antibiotics on the separated adsorbent is complete. If it cannot be effectively treated, it will still cause harm to the environment[12]. Therefore, the physical treatment technology has some limitations in the actual treatment of antibiotic wastewater.

### **1.1.2 Biological method**

Biological process[13] is the most common and efficient technology to remove organic pollutants in water treatment process. The common processes include aerobic[14], anaerobic[15] and anaerobic/aerobic[16] combined treatment. Microorganisms take pollutants as food and oxidize and decompose them, so as to realize the degradation process. Activated sludge process is a mature aerobic process, which is realized by the degradation of organic matter by microorganisms in high dissolved oxygen environment. Compared with physicochemical method, biochemical method has the advantages of high efficiency, energy saving and low

cost. It is widely used in industrial sewage treatment. Moreover, only biochemical method can effectively remove COD and greatly reduce COD value. However, there are two problems in the removal of antibiotics by biological method. One is the limitation of biological method on the removal rate and treatment cycle of refractory organics, and the other is the environmental risk of biological treatment. Zhao et al. used A/O-MBR to treat sulfamethoxazole and norfloxacin in sewage. The results show that the removal of antibiotics is mainly through degradation and partial adsorption, and the addition of easily degradable substrates such as carbon source in the biodegradation process will inhibit the degradation of antibiotics. The research shows that the parameter setting of biological treatment process is an important limiting factor for the removal of antibiotics, such as the domestication degree of sludge and sludge age (SRT). In the study of Gobel[17]and others on the removal of antibiotics in sewage, it was found that the concentrations of clarithromycin and trimethoprim were almost unchanged when SRT was 20 days, and could be removed only when SRT was more than 50 days. In addition, in the long run, there is a potential risk of enhancing resistance genes and producing "superbacteria" when using biological methods to treat antibiotics[18].

### **1.1.3 Advanced oxidation technology**

In recent years, due to the direct mineralization of refractory organic pollutants, the application of chemical treatment technology in the treatment of antibiotic wastewater has attracted extensive attention, especially advanced oxidation processes (AOPs)[19-22]. Advanced oxidation technology refers to the strong oxidizing free

radicals (including HO• and SO<sub>4</sub><sup>-</sup>• etc.) produced after a series of reactions. These free radicals directly react with organic pollutants, resulting in the breaking of their chemical bonds, or react with organic pollutants such as electron transfer, addition and substitution, so as to decompose organic pollutants into degradable small molecular substances, or even complete mineralization [23]. AOPs are generally divided into the following categories: (1) Fenton and Fenton like oxidation; (2) Photochemical and photocatalytic oxidation; (3) Ozone oxidation; (4) Ultrasonic oxidation method; (5) Electrochemical method, etc.

The research on advanced oxidation technology based on hydroxyl radical originated from the traditional Fenton method. The Fenton reaction was first discovered by French scientist h. Fenton in a scientific research in 1894. He found that the oxidation rate of tartaric acid was significantly accelerated after adding H<sub>2</sub>O<sub>2</sub> and Fe<sup>2+</sup> to tartaric acid aqueous solution. Later, people realized that the essence of Fenton reaction is that H<sub>2</sub>O<sub>2</sub> can produce a large amount of •OH under the catalysis of Fe<sup>2+</sup>, which can interact with organic pollutants to degrade organic compounds. The specific reactions are as follows:



According to the mechanism of Fenton reaction, the highly active hydroxyl radical produced by Fe<sup>2+</sup> catalyzed H<sub>2</sub>O<sub>2</sub> has an oxidation potential slightly lower than that of fluorine (2.87V). The hydroxyl radical with high oxidation potential can quickly destroy and decompose organic matter without causing secondary pollution.

Pesticides It plays an extremely important role in the degradation and removal of organic pollutants such as phenols and dyes. Grcic et al.[23] used homogeneous Fenton Method to catalyze the oxidation of 1, 2-Dichloroethane simulated wastewater. The research shows that the Fenton system has the best degradation effect on 1,2-Dichloroethane simulated wastewater after 120 min of reaction at  $\text{pH} \approx 3.0$ , and the maximum mineralization degree in the reaction system can reach 94%. Zazo et al. [24] treated phenol wastewater by Fenton method. The research shows that under the condition of  $\text{pH} = 3$ , the degradation rate of phenol in the system can reach 90% after 30 minutes of reaction. Through further detection and analysis of the degradation products after reaction, it can be found that the initially generated Pyrogallol in the reaction system finally decomposes into small molecular acids such as formic acid and acetic acid with the further reaction, This shows that Fenton system has high mineralization of phenol.

Although the traditional Fenton process has the characteristics of fast oxidation speed and simple operation, it also has many disadvantages: 1) the dosage of  $\text{H}_2\text{O}_2$  is large, the utilization rate is not high and the treatment time is long; 2) The reaction is required to be carried out under the condition of strong acidic pH, and the actual wastewater is almost neutral, so it is necessary to add acidic substances to adjust the pH, which greatly increases the experimental cost; 3) The existence of  $\text{Fe}^{2+}$  can easily lead to the problem of iron aggregation and sedimentation in the reaction process[25, 26]. The organic intermediates generated in the catalytic degradation process are easy to react with them to form stable complexes, which inhibits the further reaction between the intermediates and hydroxyl radicals, thus greatly reducing the mineralization of the

reaction. Based on the above reasons, in recent years, people have tried to combine external energy such as light, electricity, microwave and ultrasound with Fenton system, and explore to find other transition metals that can replace  $\text{Fe}^{2+}$  to participate in the reaction. We collectively call this kind of reaction Fenton like reaction. The introduction of external energy can greatly reduce the amount of Fenton reagent and significantly improve the reaction rate.

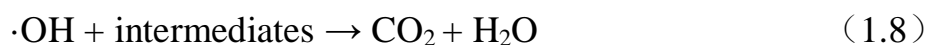
Lapertot Milena et al. [27] showed that UV Fenton method can effectively degrade some difficult biodegradable organic pollutants in pesticide wastewater. Monteagudo et al. [28] used UV Fenton system to catalyze the oxidation of reactive blue 4 and compared the degradation effects of reactive blue 4 under different reaction conditions. The results showed that when  $\text{pH} = 3$ , the combination of ultrasound and UV Fenton method had the best degradation effect on Reactive Blue 4, and the TOC removal rate was as high as 94%. Yang et al. [29] introduced microwave technology into Fenton system to treat high concentration pharmaceutical wastewater. The results show that under the conditions of  $\text{pH} = 4.42$ ,  $\text{H}_2\text{O}_2$  and  $\text{Fe}^{2+}$  concentrations of 1300mg/L and 4900mg/L respectively and microwave power of 300W, after 6min radiation, the removal rate of COD in the reaction system can reach 57.53%, and the value of  $\text{BOD}_5/\text{COD}$  is also 0.305 higher than before.

Although homogeneous Fenton technology significantly accelerates the catalytic oxidation rate compared with simple homogeneous Fenton technology, it still has some disadvantages.  $\text{Fe}^{2+}$  and  $\text{Fe}^{3+}$  remain in the reaction solution after the reaction, which is not easy to recover and easy to cause secondary pollution. Therefore, more and more

researchers begin to pay attention to the immobilization technology of  $\text{Fe}^{2+}$ . Chih et al. [30] used zero valent iron (ZVI) as a catalyst to synergistically degrade active black 5 under the action of ultrasound. The research shows that under the conditions of 60KHZ and 120W/L, at the initial pH, the dosage of ZVI and  $\text{H}_2\text{O}_2$  of 3.0, 1g/L and  $1.03 \times 10^{-2}$  mol/L, respectively, the decolorization rate of the solution can reach 99% after 10min. At the same time, ZVI can be reused for many times, and the decolorization efficiency does not decrease significantly with the reuse of ZVI. Pan et al. [31] studied the degradation of phenol by magnetic  $\text{Fe}_2\text{O}_3\text{-ZrO}_2$  catalyst under neutral conditions. The results show that the catalyst has good catalytic degradation effect on phenol under neutral conditions and the reaction system temperature is  $60^\circ\text{C}$ . After 210 min of reaction, phenol can be completely removed, and the TOC removal rate can reach 56%. At the same time,  $\text{Fe}_2\text{O}_3\text{-ZrO}_2$  has good ferromagnetism, which is helpful to further recycle the catalyst. Wang et al. [32, 33] studied the Fenton like system composed of nano solid  $\text{Fe}_3\text{O}_4$  as catalyst and  $\text{H}_2\text{O}_2$  as oxidant, and investigated the catalytic degradation performance of the system for azo dye rhodamine B. The results show that the suitable pH of nano  $\text{Fe}_3\text{O}_4$  catalyst is wide. When  $\text{pH} = 3\text{-}9$ , the catalyst can efficiently activate  $\text{H}_2\text{O}_2$  to achieve better treatment effect of rhodamine B. Xu et al. [34] prepared heterogeneous catalyst  $\text{Fe}^0$  and applied it to catalytically activated  $\text{H}_2\text{O}_2$  degradation of 4-cis-3-methylbenzoic acid (CMP). The effects of different pH,  $\text{H}_2\text{O}_2$  Content, CMP concentration and catalyst content on the experimental results were studied. The results showed that the optimum experimental conditions of the catalytic system were  $\text{pH} = 6.1$ ,  $\text{Fe}^0$  and CMP concentrations were 0.5g/l and 0.7mmol/l respectively,  $\text{H}_2\text{O}_2 = 3\text{mmol/L}$ , At the same

time, it is also found that compared with the homogeneous reaction system, the application range of pH in the heterogeneous reaction system is wider.

Photochemical oxidation refers to a method in which oxidants (such as H<sub>2</sub>O<sub>2</sub>[35], O<sub>3</sub>, ClO<sub>2</sub>[36], etc.) decompose into •OH under the action of ultraviolet light (or visible light), and organic pollutants degrade and remove under the strong oxidation of •OH. UV/H<sub>2</sub>O<sub>2</sub> method[37] is widely used in this method. Under UV irradiation, H<sub>2</sub>O<sub>2</sub> will decompose into two •OH. The generated •OH can continue to react with the remaining H<sub>2</sub>O<sub>2</sub> in the reaction to form another free radical (HO<sub>2</sub>•). The •OH generated in the reaction process can not only oxidize the organic pollutants in the system, but also further oxidize the organic intermediates. The above reaction process is as follows:



In 1975, Koubek et al. [38] first used the method of combining UV and H<sub>2</sub>O<sub>2</sub> to improve the degradation efficiency of the reaction system. The combination of the two makes H<sub>2</sub>O<sub>2</sub> decompose to produce •OH, and use its strong oxidation to effectively degrade organic pollutants. Chen [39] compared and studied the degradation effect of dioctyl phthalate (DEHP) in water by UV and H<sub>2</sub>O<sub>2</sub> combined method and single UV

illumination method. The results showed that UV/H<sub>2</sub>O<sub>2</sub> method was more effective than single UV illumination method in oxidative degradation. After 180min reaction, the removal rates of DEHP by UV/H<sub>2</sub>O<sub>2</sub> method and single UV illumination method were 100% and 73.5% respectively. Yu studied the degradation ability of Typical Antibiotics by photochemical method. The research shows that the degradation rate of sulfamethoxazole (SMX) is directly proportional to the UV irradiation intensity and inversely proportional to the pH value in the system. Although SMX can achieve high degradation rate under UV irradiation alone, the mineralization degree in the whole reaction system is very low. The introduction of H<sub>2</sub>O<sub>2</sub> not only significantly improves the degradation rate of SMX, but also greatly enhances the mineralization degree in the whole system. The reason is that highly active •OH is produced in the reaction process, which directly interacts with SMX to enhance the degradation effect of organic matter. When the H<sub>2</sub>O<sub>2</sub> concentration is 10mm, after 8h reaction, the COD removal rate in the solution can reach more than 80%. Xu et al.[40] pointed out that neither UV nor H<sub>2</sub>O<sub>2</sub> alone can effectively degrade diethyl phthalate (DEP), while UV/H<sub>2</sub>O<sub>2</sub> technology can achieve efficient degradation of dep. the research shows that when the UV intensity is 133.9 μ Under the condition of W/cm<sup>2</sup> and H<sub>2</sub>O<sub>2</sub> dosage of 20mg/L, the degradation rate of DEP exceeded 98.6% within 1h.

Photocatalytic oxidation technology [41-43] is a research hotspot in sewage treatment. It has many advantages, such as short reaction time, non-toxic and high catalytic efficiency. Photocatalytic oxidation technology is developed based on photochemical oxidation technology. The reaction of photochemical oxidation technology mainly refers to the process that organic pollutants are gradually oxidized

and degraded by ultraviolet irradiation. However, due to the limitations of various reaction conditions, its oxidative degradation is usually not complete enough, which has become a difficult problem to be overcome by this technology. In order to significantly enhance the efficiency of this oxidation technology, researchers put forward the idea of combining it with photocatalyst, and defined this kind of method as photocatalytic oxidation. Among them, homogeneous photocatalytic oxidation uses  $\text{Fe}^{2+}$  or  $\text{Fe}^{3+}$  as catalyst to produce more  $\cdot\text{OH}$  through photo assisted Fenton reaction to degrade pollutants. Heterogeneous photocatalytic oxidation uses some semiconductor materials as photocatalysts (such as  $\text{TiO}_2$ ,  $\text{ZnO}$ , CDs,  $\text{WO}_3$ , etc.), which can produce photogenerated holes ( $\text{H}^+$ ) with strong oxidation and photogenerated electrons ( $\text{e}^-$ ) with strong reduction under UV irradiation, and use their respective oxidation and reduction characteristics to generate a series of active free radicals, such as  $\cdot\text{OH}$ ,  $\text{O}_2^{\cdot-}$  and  $\text{HO}_2\cdot$ . These highly active free radicals are used as organic pollutants to convert them into carbon dioxide, water or other biodegradable small molecular substances, so as to remove organic pollutants efficiently. Therefore, photocatalytic oxidation technology is widely used in the treatment of various organic wastewater.

In the process of photocatalytic oxidation degradation of organic pollutants in water,  $\text{TiO}_2$ , as a semiconductor catalyst, has good catalytic effect and is widely used. The basic principle of the reaction is as follows:





Zhou et al.[44] prepared N-I Co doped anatase nano-TiO<sub>2</sub> by hydrolysis method to catalyze the degradation of methyl orange (MO) wastewater. The research shows that n-i co doping can reduce the band gap of TiO<sub>2</sub> and enhance the light absorption in the range of 400-600nm, so it has higher visible photocatalytic activity than TiO<sub>2</sub>. After visible light irradiation for 2h, the decolorization rate was 96.3%, and after UV visible light irradiation for 4h, the COD removal rate was 41.7%. Although photocatalytic oxidation is an economic and clean technology, there are some problems, such as complex preparation process and difficult recovery of most catalysts, and it is difficult to achieve good treatment effect for high turbidity wastewater with poor light transmission.

Electrochemical oxidation [45-49] is a new advanced oxidation technology that uses the active substances generated by the action of electrodes to react with organic pollutants to achieve rapid oxidative degradation. Electrochemical oxidation has a good treatment effect on some organics that are difficult to biodegrade. Its core reaction process can be divided into two categories. One is direct oxidation. Its action mode is that organics are adsorbed on the anode surface and  $\cdot\text{OH}$  is generated by water molecules discharging on the anode surface, which can directly oxidize organic

pollutants; the other is indirect oxidation. The electrode material first reacts to produce  $\text{MOX} + 1$ , and then uses its strong oxidation to effectively remove organic pollutants. Because the electrochemical oxidation method is easy to operate and easy to control, and no other catalysts are introduced in the reaction, it will not lead to the problem of secondary pollution. Therefore, this technology is an effective method to treat toxic, harmful, high salt and high concentration organic wastewater.

Samihahammami et al. [50, 51] used electrochemical oxidation technology to treat azo dyes. The results showed that under the optimal conditions, the dye solution could be almost completely mineralized after 6h (TOC removal rate was as high as 98%). Radha et al.[52] studied the treatment effect of electrochemical oxidation method (graphite rod as anode and stainless steel as cathode) on textile industry wastewater. The research shows that under strong acid conditions, when the current density is  $28\text{mA}\cdot\text{cm}^{-2}$ , the removal rates of COD and TOC are 68% and 96.8% respectively, and the color removal rate of waste liquid can reach 96%. Although electrochemical oxidation technology has incomparable advantages over other water treatment technologies, due to the continuous power consumption of electrochemical oxidation technology, it can not be popularized and used on a large scale in practical application at this stage.

The redox potential of ozone [53, 54] can be as high as 2.08V. Advanced oxidation technology, which is used as oxidant because of its strong oxidation ability, has developed rapidly in recent years. This technology is widely used in environmental protection and chemical industry. Ozone in water treatment can not only sterilize, remove peculiar smell and odor, but also destroy the structure of organic matter.

In the application process of oxidative degradation of organic pollutants in water, the reaction process between ozone and organic matter can be roughly divided into two types: one is that ozone can directly oxidize organic matter, and the other is that ozone first decomposes to produce  $\bullet\text{OH}$ , and then reacts with organic matter in water, so as to achieve the purpose of degradation and removal of organic matter.

$\text{O}_3$  will produce  $\bullet\text{OH}$  in alkaline solution, which can effectively remove organic pollutants. Somensi et al.[55] applied ozone oxidation method to the pretreatment of printing and dyeing wastewater. The research results show that under acidic conditions, the removal rates of chromaticity and COD of wastewater after 4h are 40.6% and 18.7% respectively. Under alkaline conditions, the removal rates of chromaticity and COD are significantly improved, and the biodegradability of wastewater (BOD/COD) is improved. It also increased from 0.06 to 0.41.

At present, the advanced oxidation technology for treating pollutants in water mainly uses  $\text{HO}\bullet$  and  $\text{SO}_4\text{-}\bullet$  as the main free groups to oxidize and degrade pollutants. In recent years, peroxide based advanced oxidation technology has been widely used in the field of organic pollutant removal, including inorganic peroxides dominated by calcium peroxide (CP) and organic peroxides dominated by peracetic acid (PAA).  $\text{HO}\bullet$  and other free groups are catalyzed by body and activator.  $\text{HO}\bullet$  is a strong oxidant and has high redox potential ( $E^0 = 2.73\text{V}$ ). In recent years, based on the rise of persulfate advanced oxidation system,  $\text{SO}_4\text{-}\bullet$  has strong oxidation capacity for pollutants, and its oxidation activity can adapt to a wider pH range. However, the problem of sulfate pollution caused by the removal of pollutants can not be ignored. With the development of persulfate advanced oxidation system with oxides as the main oxidant

are widely used, how to activate peroxides to accelerate the removal of pollutants has become a research hotspot. At present, the main activation methods of peroxides are ultraviolet light, transition metals and carbonaceous materials. Based on the aspects of high efficiency, green and practicability, transition metals and carbonaceous materials are widely used as the main activators.

## **1.2 Overview of peroxide advanced oxidation system**

Peroxide is a compound containing peroxy-O-O-, which can be regarded as a derivative of hydrogen peroxide, and its characteristic is the presence of peroxy ion in the molecule. Peroxides are divided into inorganic peroxides and organic peroxides, mainly including hydrogen peroxide, calcium peroxide and peracetic acid. At present, peroxide is widely used in textile industry, bleaching industry and environmental pollution remediation.

### **1.2.1 Hydrogen peroxide**

Hydrogen peroxide[56, 57], also known as hydrogen peroxide (HP), is a colorless and transparent liquid with strong water solubility and can be miscible with water in any proportion. Hydrogen peroxide solution with a content of about 30% is used most frequently. There are many preparation processes of hydrogen peroxide. At present, anthraquinone method is the main method. Hydrogen peroxide has been widely used in various fields because of its oxidation, bleaching and disinfection effects. As an oxidant, the hydroxyl radical (HO•) produced by HP can combine with pollutants without selectivity to degrade pollutants.

### **1.2.2 Calcium peroxide**

Calcium peroxide[58-60], also known as calcium dioxide ( $\text{CaO}_2$ ), a white or light yellow crystalline powder, is a more general and safe solid inorganic peroxide at present. It is considered to be the "solid form" of hydrogen peroxide ( $\text{H}_2\text{O}_2$ ). The commonly used preparation methods are calcium chloride method and calcium hydroxide method. In the natural state, dissolving  $\text{CaO}_2$  in water can slowly release  $\text{H}_2\text{O}_2$  and oxygen ( $\text{O}_2$ ) at a "controlled" rate, effectively reducing the occurrence of disproportionation reaction, and 1 g of  $\text{CaO}_2$  can release up to 0.47g of  $\text{HO}$ . The release rate of  $\text{HO}$  mainly depends on the dissolution rate of  $\text{CaO}$  and is greatly affected by the pH of water body. Compared with other compounds that can produce  $\text{H}_2\text{O}_2$  (such as  $\text{Na}_2\text{CO}_3$ ,  $\text{MgO}_2$ , etc.),  $\text{CaO}_2$  is cheaper and has a long history of application in field repair. In recent years, the application of  $\text{CaO}_2$  instead of  $\text{H}_2\text{O}_2$  has also been frequently reported. In addition to its stable oxidation capacity,  $\text{CaO}_2$  also has the functions of bleaching, deodorization and disinfection. It has been widely used in agriculture, aquaculture, pharmaceutical industry and other fields.

$\text{CaO}_2$  has good oxygen release characteristics and its own non-toxic and harmless green performance. As an oxygen supply agent,  $\text{CaO}_2$  is widely used in aquaculture[61], crop cultivation[62] and sewage treatment [63]; Ndjou'ou and Cassidy [64] observed that the degradation rate of pollutants based on  $\text{CaO}_2$  oxidation reaction was increased by at least 20% compared with liquid  $\text{H}_2\text{O}_2$ . Some studies have also reported the use of  $\text{CaO}_2$  to remove various pollutants. Goi et al. [65] applied  $\text{CaO}_2$  to treat the soil polluted by electrical insulating oil containing polychlorinated biphenyls, which can achieve an oil degradation rate of  $(96 \pm 2\%)$ ; Zhang et al. found that in the pH range of 2-12,  $\text{CaO}_2$  alone can effectively remove six phenolic endocrine

disrupting compounds from activated sludge; Li et al. also proved that  $\text{CaO}_2$  can effectively remove organic pollutants that are not biodegradable under ordinary anaerobic conditions. In addition, it also has good effects in removing other pollutants, including organic pollutants such as 2,4,6-trinitrotoluene (TNT)[66], polycyclic aromatic hydrocarbons (PAHs)[67], trichloroethylene (TCE)[68].

### **1.2.3 Peracetic acid**

Peracetic acid[69-71] (PAA) is an organic peroxide with strong pungent smell. At present, the more common commercial PAA solution is a mixture containing PAA, acetic acid, hydrogen peroxide and water. As the solution containing more than 15% PAA has a certain degree of explosion, instability and overreaction, the concentration of PAA needs to be diluted according to the needs of application. As a disinfectant and oxidant, PAA is widely used in medical facilities, agricultural facilities, food enterprises, beverage processing plants and textile industry because of its high efficiency and low toxicity.

As a strong oxidant, PAA has the characteristics of low toxicity and less by-products; As a weak acid, the dissociation constant  $\text{pK}_a$  of PAA is 8.2. When pH is lower than 8.2, PAA is considered to spontaneously decompose viable oxygen, which can destroy sulfhydryl (-SH) and sulfur bond (S-S) in enzymes and proteins in cell membrane. As a disinfectant, the main advantage of PAA relative to chlorine based disinfectant is that it can react and decompose quickly, which may eliminate the need for quenching before discharge. It is reported that when PAA reacts with wastewater or natural organic matter, it produces little or no toxic by-products. At the

same time, PAA has been proved to be an effective alternative to treat contaminated wastewater with lower dose and shorter reaction time, and can be used to treat CSO [72-74]. At present, the research has solved the problem of disinfection of wastewater by PAA, but researchers found that the effective dose and exposure time of PAA vary greatly due to water quality. As a new type of organic peroxide, PAA can produce more free groups because of its low peroxide bond energy ( $38 \text{ kcal} \cdot \text{mol}^{-1}$ ). At present, advanced oxidation technology using PAA as oxidant has also achieved good results in pollution control such as phenols[75], dyes and antibiotics[76-78].

#### **1.2.4 Potassium bisulfate ( $\text{KHSO}_5$ )**

Unlike symmetric peroxides[79-82] such as  $\text{K}_2\text{S}_2\text{O}_8$  and  $\text{H}_2\text{O}_2$ ,  $\text{KHSO}_5$  (potassium peroxyphosphate, PMS) is an asymmetric peroxide formed by replacing  $\text{HOOH}$  with  $\text{SO}_3^-$ . Its unique structure also makes it easy to be excited and activated. Oxone is a commercial form of  $\text{KHSO}_5$ . It is a composite salt (i.e.  $\text{KHSO}_5 \cdot \text{KHSO}_4 \cdot \text{K}_2\text{SO}_4$ ) composed of a molecule of  $\text{KHSO}_5$ , a molecule of  $\text{KHSO}_4$  and a molecule of  $\text{K}_2\text{SO}_4$ . The effective component is  $\text{KHSO}_5$ . Oxone is a kind of granular white powder with good fluidity. Because of its stable properties, easy treatment, non-toxic, diverse functions and low cost, oxone is widely used in the field of organic synthesis as an oxidant, such as olefin epoxidation[83], paraffin epoxidation[84], bromination, decarbonylation of phenylacetic acid, selective oxidation of benzyl alcohol compounds[85], etc. In the field of disease prevention and control, oxone was used in Europe to control foot-and-mouth disease virus (FMD) in 2001[86]. Antec company produced a powerful bactericide virkons with PMS as the active ingredient,

which was approved as a drug for the prevention and control of FMD by the Ministry of agriculture, fisheries and food of the UK[87]. In addition, oxone as a disinfectant is also highly sensitive to chicken avian influenza[88], chicken infectious bronchitis[89] and chicken Marek's virus[90]. In the field of water treatment, oxone can not only kill microorganisms through its oxidation, but also remove organic matter in water. Dissolved in water, free radicals and reactive oxygen species of various high-energy and high-activity small molecules are produced, which can destroy the permeability barrier of microbial cell membrane, resulting in loss of cell content logistics and loss of the function of energy-dependent membrane transport system, and can combine with metal ions such as calcium and iron in nucleic acid to produce active free radicals, which act on the phosphodiester bond of DNA and cause its breakage, It also has a similar destructive effect on RNA, and there is no harmful residue in nature after degradation. In addition, oxone disinfection does not produce disinfection by-products (DBPs) such as monochloromethane, dibromomono-chloromethane, chloroform and other organic halogenates. Therefore, oxone has replaced Cl<sub>2</sub> as a disinfectant for drinking water treatment in some countries. In addition, PMS is also used as a disinfectant for swimming pools[91], a cleaning and etching agent for printed circuit boards[92], and an assistant for repulping and fiber reconstruction of wet strength paper[93].

### **1.3 Advanced oxidation technology based on persulfate**

#### **1.3.1 Activation mechanism of Fenton like catalytic system based on hydrogen persulfate**

The advanced oxidation process based on  $\text{SO}_4^{\cdot-}$  has attracted extensive attention because of its strong degradation ability of refractory organic pollutants [38][79, 80, 82]. Both persulfate (PS,  $\text{S}_2\text{O}_8^{2-}$ ) and hydrogen persulfate (PMS,  $\text{HSO}_5^-$ ) can produce  $\text{SO}_4^{\cdot-}$ .  $\text{SO}_4^{\cdot-}$  and  $\cdot\text{OH}$  are strong oxidants, which can effectively degrade pollutants. Compared with the traditional Fenton reaction, the Fenton like catalytic system based on sulfate has a series of advantages, such as higher oxidation potential, better selectivity and efficiency, oxidation of pollutants containing unsaturated bonds or aromatic rings, and wider pH application range [39]. In addition, in some cases,  $\text{SO}_4^{\cdot-}$  has higher selectivity and longer half-life than  $\cdot\text{OH}$  [40].

### **1.3.2 Activation method of Fenton like catalytic system based on hydrogen persulfate**

At present, the commonly used PMS activation methods mainly include heating activation, radiation activation, alkali activation, catalytic activation, etc.[94-96]. Heating method is a very effective way of catalytic activation.

#### **(1) Thermal activation**

The research shows that PMS can be catalytically activated at room temperature (22 °C). The heating method mainly depends on increasing the system temperature to accelerate the oxygen bond breaking reaction of PMS in aqueous solution (reaction formula 1-16) [82]. Increasing the reaction temperature can improve the activation efficiency of PMS, but the solubility of some organic compounds also increases when the temperature increases, which is not very suitable for the advanced treatment of dye wastewater. In addition, during the heating process, it is easy to cause  $\text{SO}_4^{\cdot-}$

quenching, which affects the progress of organic degradation reaction. Yang [97] et al. used thermally activated PMS to degrade azo dye Acid Orange 7 (AO7). It was found that AO7 was more easily degraded by PMS at high temperature (80 °C) than at low temperature. Antoniou[98] et al. found that PMS is easier to be activated by heating than PS and H2O2 when using thermally activated PMS to remove LR microcystins.



## (2) Radiation activation

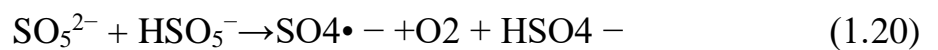
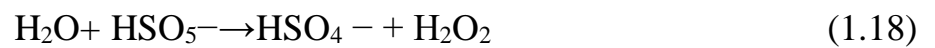
Radiation activation mainly depends on ultrasound, ultraviolet and light  $\gamma$  X-ray radiates the reaction system and uses the radiation energy to promote the decomposition of PMS (reaction formula 1-17). Compared with the other two methods, ultraviolet radiation activation is considered to be a more promising method for safety and economy. Verma found in the degradation of Anabaena toxin by UV activated PMS at  $\lambda = 260$  nm, UV showed the best activation performance. During the study, Lei found that the primary and secondary radicals generated by UV/PMS system in complex water environment play an important role in the degradation of diethyl phthalate. However, the proportion of ultraviolet light in natural light is only 8.7%, which limits the popularization and application of this technology.



## (3) Alkali activation [99-101]

The reaction solution with alkaline pH in the system can also effectively catalyze and activate PMS to produce  $\text{SO}_4^{\bullet-}$ . This is because under alkaline

conditions, PMS will first decompose into hydrogen peroxide, and then react with the generated hydrogen peroxide to produce  $\text{SO}_4^{\cdot-}$ . In addition, PMS can generate  $\text{SO}_4^{\cdot-}$  [47] by self decomposition. However, this technical means needs to continuously add drugs to adjust the pH of the system, the operation is complex and the economy is not high, so there are few studies on the degradation of organic pollutants. The specific reaction formula involved in the catalytic activation technology is as follows:



#### (5) Carbon material activation

Carbon materials can also effectively activate PMS. In the process of catalytic activation of PMS, it mainly uses the electron transfer of the system to achieve its purpose. The electrons in the carbon material are extracted during the reaction and supplied to PMS as the raw material for generating  $\text{SO}_4^{\cdot-}$  (reaction formula 1-21)[102-105]. Some studies have also shown that non free radicals also make some contributions in the degradation of organic matter by carbon activated PMS (reaction formula 1-22). However, in the actual experiment, it is found that due to the large specific surface area and strong adsorption capacity of carbon material, it will adsorb organic pollutants on the material surface during the reaction process, hinder the transfer of electrons, and then affect the degradation reaction of the system. In addition, after adsorbing organic pollutants on the surface of carbon based materials,

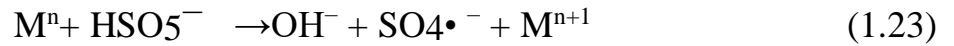
its reuse performance will also be affected, which will also limit its practical application.



#### (6) Metal ion activation

The catalytic activation of PMS by metal ions is mainly realized by electron transfer of redox reaction pairs formed by transition metal elements (reaction formula 1-8), which usually includes homogeneous metal ion catalytic activation and heterogeneous metal compound catalytic activation. At present, the commonly used transition metals mainly include iron[106, 107], manganese[108-110], copper[111, 112], nickel[113, 114], cobalt[115-117] and silver[118, 119]. Bouzayani[120] et al. compared the activation effects of Co, Cu, Ni and Fe plasma on PMS, and concluded that Co ions showed the best activation effect on PMS. Pan [121] et al. used MoS to enhance the activation ability of homogeneous  $\text{Co}^{2+}$  ions to PMS. The removal rate of Rh B was increased by 45% in 5 min. it was also concluded that the pH of the solution had an important impact on the catalytic activation effect of the system. However, the homogeneous catalytic system has many disadvantages, such as the difficulty of metal ion recovery, the need for continuous readdition, and some heavy metal ions are easy to form secondary pollution to the environment. Compared with the homogeneous system, the heterogeneous catalytic system benefits from the catalytic materials with fixed forms. The metal ions are not easy to be lost and the materials are easy to be recycled. In addition, its activation ability can be improved

through the composite of different materials. Li et al. used CoFe<sub>2</sub>O<sub>4</sub>[122] to activate PMS to decompose herbicide atrazine, analyzed its reaction kinetics and decomposition mechanism, and achieved good experimental results.



Based on the above discussion on the activation mode of PMS, multiphase metal compounds are selected as the activator of PMS for the next experiment. According to the previous research results, the catalytic materials formed by a variety of transition metal elements have good activation ability for PMS, such as Co, Cu, Ni, Fe, etc. among them, cobalt has been widely studied because of its high catalytic activity.

## **1.4 Co/PMS catalytic oxidation system**

### **1.4.1 Introduction to CO/PMS catalytic oxidation system**

As we all know, the traditional advanced oxidation technology, especially the Fenton technology based on hydroxyl radical, has some disadvantages, such as high requirements for pH value range, large amount of Fe<sup>2+</sup> not participating in the reaction, low degree of mineralization of organic matter, large amount of iron sludge to be treated, oh is easy to be quenched and inactivated. The Co/PMS system based on sulfate radical is a new advanced oxidation technology based on Fenton like reaction to overcome the above shortcomings of Fenton technology. SO<sub>4</sub><sup>•-</sup> technology using Co/PMS system to produce strong oxidation activity was first applied in inorganic and biochemical fields. It was not until 2003 that Anipsitakis[123]of Ohio State University applied the Co/PMS system to the field of environment for the first

time. Anipsitakis and others have just found that among many transition metal ions,  $\text{Co}^{2+}$  is the most efficient metal ion to activate PMS to produce  $\text{SO}_4^{\cdot-}$  through experiments.

Co/PMS system is a kind of Fenton reaction system, which uses transition metal  $\text{Co}^{2+}$  to catalyze and activate PMS to produce oxidizing free radical  $\text{SO}_4^{\cdot-}$  with stronger activity than  $\cdot\text{OH}$ , and then uses  $\text{SO}_4^{\cdot-}$  to degrade organic pollutants in water, so as to achieve the purpose of wastewater treatment. The Co/PMS system can show high oxidation activity in the pH range of 3 ~ 8, and the amount of cobalt is small, which overcomes the shortcomings of Fenton reaction. Therefore, Co/PMS system has been widely used. According to the different states of transition metal cobalt in the system, the Co/PMS system is divided into homogeneous and heterogeneous Co/PMS catalytic oxidation systems. In the homogeneous Co/PMS catalytic oxidation system, cobalt exists in the form of cobalt ions, that is, cobalt ions are directly introduced into the reaction system; In heterogeneous Co/PMS catalytic oxidation system, cobalt exists in the form of supported or unsupported cobalt oxide.

The generation of sulfate radical from PMS catalyzed by cobalt began in 1958. Since then, a large number of studies on the generation of free radical oxidation of organic pollutants by PMS activated by transition metals have been carried out, but the research results show that cobalt is the best catalyst for PMS to produce free radicals. Just as  $\text{Fe}_3\text{O}_4$  is composed of FeO and  $\text{Fe}_2\text{O}_3$ , there are two states of cobalt in  $\text{Co}_3\text{O}_4$ , i.e.  $\text{Co}^{2+}$  in CoO and  $\text{Co}^{3+}$  in  $\text{Co}_2\text{O}_3$ . According to the research of Dionysiou et al., the dissolution of cobalt ions in CoO in solution state is much more

than that of  $\text{Co}_3\text{O}_4$ . Under acidic conditions,  $\text{CoO}$  dissolves a large amount of  $\text{Co}^{2+}$ , so  $\text{CoO}$ /The PMS system is homogeneous. The dissolution of cobalt in  $\text{Co}_3\text{O}_4$  is due to the presence of  $\text{CoO}$  in its composition. Therefore,  $\text{Co}_3\text{O}_4$  has catalytic effect, which is caused by the dissolution of cobalt in  $\text{CoO}$ , while the dissolution of cobalt in  $\text{Co}_2\text{O}_3$  is very little. In addition, the reduction ability of metals from oxidation state to reduction state or the metal in hydrolysis and coordination will be produced in the activated oxidant in the oxidation state. Free radicals and matrix play an important role in the transformation reaction. The hydrolysis products of single or multi nuclei play a good role in the electron transfer reaction.

#### **1.4.2 Homogeneous Co/PMS catalytic oxidation system**

The application of homogeneous Co/PMS system is very convenient. Just add a small amount of  $\text{Co}^{2+}$  to the reaction system with oxidant PMS, and  $\text{Co}^{2+}$  can quickly activate PMS to produce strongly active  $\text{SO}_4^{\cdot-}$ . Due to the convenience of homogeneous Co/PMS system, the system has been widely studied and applied. Dionysion et al. [123] studied the degradation of 2,4-Dichlorophenol by Co/PMS system and compared it with Fenton system. The results show that the degradation effect of Co/PMS system on 2,4-Dichlorophenol is much better than Fenton at pH 2-9. Wang et al. [124] studied the effects of different cobalt salts such as  $\text{Co}(\text{NO}_3)_2$ ,  $\text{CoSO}_4$ ,  $\text{CoCl}_2$  and  $\text{Co}(\text{CH}_3\text{COO})_2$  on the degradation of atrazine in Co/PMS system. The results confirmed that  $\text{CoCl}_2$  had obvious inhibitory effect. Bandala et al. [125] used CO/PMS system to degrade 2, 4-D under light conditions. The results show that light is conducive to the degradation reaction. Chen et al. [126] studied the

effects of inorganic ions such as  $\text{H}_2\text{PO}_4^-$ ,  $\text{HCO}_3^-$ ,  $\text{NO}_3^-$  and  $\text{Cl}^-$  in the degradation of insecticide imidacloprid by Co/PMS system on the degradation efficiency. The results showed that  $\text{H}_2\text{PO}_4^-$  and low concentration of  $\text{HCO}_3^-$  promoted the degradation reaction,  $\text{Cl}^-$  and high concentration of  $\text{HCO}_3^-$  inhibited the reaction, and  $\text{NO}_3^-$  had little effect on the reaction. Chen et al. [127] also deduced the reaction kinetic model of degradation of AO7 by Co/PMS system, which showed that the reaction was consistent with Quasi first order reaction kinetics. Anipsitakis[123] et al. studied the intermediate products of phenol compounds degraded by  $\text{Co}^{2+}$  + activated persulfate and the effects of chloride ions. The research shows that the intermediate products of 2, 4-Dichlorophenol degraded by this system are 2,4,6-trichlorophenol, 2,3,5,6-tetrachloro-1,4-hydroquinone, 1,1,3,3-tetrachloroacetone, etc., and the presence of chlorine may lead to the chlorination of organic compounds. Wang et al. [128] found that  $\text{Cl}^-$  had a great effect on the degradation of orange II in Co/PMS system when the chloride ion concentration was 0.15 ~ 10 mg/L, but promoted the reaction when the chloride ion concentration was greater than 50 mg/L. Sun et al. [129] confirmed that the removal rate of COD, SS and chromaticity in landfill leachate by homogeneous Co/PMS system is significantly higher than that of Fenton system. Matta et al. [130] found that the degradation efficiency of trace drug ritodrine in actual municipal sewage by homogeneous Co/PMS system is significantly higher than that of traditional Fenton system. Do et al. [131] used Co/PMS system to treat the eluent of diesel contaminated soil by sequential batch injection. It was found that when the molar ratio of PMS to  $\text{Co}^{2+}$  was 500:3, the diesel degradation rate could reach 90% by injection in five times.

### 1.4.3 Heterogeneous Co/PMS catalytic oxidation system

Although homogeneous Co/PMS system has many advantages, such as strong oxidation ability, high oxidation efficiency, good selectivity and wide application range, it also has some disadvantages, such as  $\text{Co}^{2+}$  is not friendly to the environment and the catalyst is not easy to recover and reuse. Especially, although the amount of  $\text{Co}^{2+}$  in homogeneous catalytic oxidation system is not large, a small amount of  $\text{Co}^{2+}$  ions discharged into the natural environment can still cause potential secondary pollution and biological toxicity. If  $\text{Co}^{2+}$  can be immobilized, that is, select a suitable carrier and fix cobalt on this carrier, so that  $\text{Co}^{2+}$  can not be lost and play a good catalytic activity, the weakness of homogeneous catalyst can be overcome. The advanced oxidation technology of heterogeneous Co/PMS system is based on this. Heterogeneous catalytic oxidation system is a complex system different from homogeneous system. Heterogeneous system has special reaction characteristics and process. The oxidation process of heterogeneous system mainly involves five steps: ① diffusion of cloth machine pollutants from liquid phase to solid phase; ② adsorption of organic pollutants on the catalyst surface; ③ catalytic reaction of metal oxides in solid phase; ④ desorption of reaction products from the catalyst surface; ⑤ The reaction product diffuses into the phase. In the above adsorption and desorption processes, the material transfer between solid phase and liquid phase plays an important role.

The results[79, 82, 132, 133] show that the catalytic effect of transition metals is in the order of  $\text{Co}^{2+} > \text{Ru}^{3+} > \text{Fe}^{2+} > \text{Ce}^{3+} > \text{V}^{3+} > \text{Mn}^{2+} > \text{Fe}^{3+} > \text{Ni}^{2+}$ , among which  $\text{Co}^{2+}$  is the best catalyst for activating PMS. Anipsitalis et al. studied the catalytic effect of two

commercial Co oxides CoO and Co<sub>3</sub>O<sub>4</sub>, and preliminarily discussed the mechanism of heterogeneous catalysis. The results show that Co<sub>3</sub>O<sub>4</sub> can catalyze PMS, and the catalytic effect is more prominent under neutral conditions. Chen et al. used the nano-sized Co<sub>3</sub>O<sub>4</sub> synthesized by them to catalyze PMS to produce sulfate radical to degrade AO7. The results show that nano-sized Co<sub>3</sub>O<sub>4</sub> can play a good catalytic activity and the dissolution of cobalt ions is very low. At the same time, Anipsitakis et al [123, 134] put forward for the catalytic mechanism: firstly, because CoO does not show catalytic performance, and Co<sub>3</sub>O<sub>4</sub> is composed of CoO and Co<sub>2</sub>O<sub>3</sub>, Co<sub>2</sub>O<sub>3</sub> really plays a catalytic role; secondly, through the comparison of the dissolution of pure CoO and Co<sub>3</sub>O<sub>4</sub> with the same Co content in solution, it is found that the dissolution of pure CoO is higher than that of Co<sub>3</sub>O<sub>4</sub>, indicating that the dissolution of CoO and Co<sub>2</sub>O<sub>3</sub> in Co<sub>3</sub>O<sub>4</sub> is higher. Therefore, it is of great significance to select the appropriate support for cobalt catalyst for heterogeneous catalytic system.

At present, a large number of studies on the application of supported cobalt catalysts to advanced oxidation technology for wastewater treatment are under way. Chu et al loaded cobalt on zeolite and cation exchange resin to activate PMS for oxidative degradation of herbicide Chlorsulfuron. The results showed that under the same conditions, when the carrier was zeolite, the degradation rate of Chlorsulfuron was 100% within 10 minutes, but the recycling effect was not good; When the carrier is cationic resin, the degradation efficiency and recycling effect are very good, and the mineralization degree of Chlorsulfuron is also very high in the presence of ultraviolet light. Yanget al selected iron oxide nanoparticles as the carrier of cobalt and compared the degradation of 2,4-dichlorobenzene between Co/TiO<sub>2</sub>/PMS system

and Co<sub>3</sub>O<sub>4</sub>/PMS system. The results showed that due to the existence of surface lifting functional groups and the uneven distribution of Co<sub>3</sub>O<sub>4</sub> at 10-15nm on the surface of TiO<sub>2</sub> at 30-40nm, the catalytic activity of Co/TiO<sub>2</sub>/PMS system was higher than that of Co<sub>3</sub>O<sub>4</sub>/PMS system. Zhang et al [136] also studied the degradation of 2,4-dichlorobenzene by activated PMS loaded with cobalt on different carriers such as Al<sub>2</sub>O<sub>3</sub>, TiO<sub>2</sub> and SiO<sub>2</sub>, and investigated the effects of carrier, cobalt precursor and ultraviolet light. Yu et al selected lachian ring as the carrier of Co<sub>3</sub>O<sub>4</sub> to activate PMS and degrade acid orange II. Shukla et al [135] loaded cobalt on three types of zeolites (A, X and ZSM-5) as heterogeneous catalysts to catalyze PMS to produce SO<sub>4</sub><sup>-•</sup> to degrade phenol. The results show that Co-ZSM-5 catalyst has the best catalytic performance, less cobalt ion dissolution and good stability. Shukla also used activated carbon (AC) as the carrier of Co<sub>2</sub>O<sub>3</sub> to prepare heterogeneous catalyst to activate PMS to degrade phenol. The research showed that when the reaction condition was 500ml phenol solution with concentration of 25ppm, adding 0.1g catalyst and 1g PMS for 60min, the degradation efficiency of phenol was 100% and the removal rate of TOC was 80%. Zhang [137] loaded Co<sub>3</sub>O<sub>4</sub> on different supports (MgO, ZnO, Al<sub>2</sub>O<sub>3</sub>, ZrO<sub>2</sub>, P25, SBA-15) to activate PMS to produce sulfate radical to degrade methylene blue (MB), acid orange II, malachite green and other organic dyes. The results showed that when Co<sub>3</sub>O<sub>4</sub> was loaded on MgO and the loading capacity was 5wt%, MB was completely degraded within 7min, and the degradation efficiency was higher than that of homogeneous CO<sub>2</sub> +/PMS and heterogeneous Co<sub>3</sub>O<sub>4</sub>/PMS. Liu [138] uses polytetrafluoroethylene (PTFE) as the carrier of nano Co<sub>3</sub>O<sub>4</sub> to make a heterogeneous catalyst to catalyze PMS to degrade organic

wastewater such as acid orange II with the aid of light. The results show that when the prepared PTFE/Co<sub>3</sub>O<sub>4</sub> is used as the catalyst to activate PMS, the degradation of Acid Orange II can be completed in a few minutes, and there is little dissolution of cobalt ions.

So far, the commonly used methods for synthesizing heterogeneous Co / PMS catalysts include wet impregnation high temperature calcination, coprecipitation, ion exchange, thermal oxidation and so on. The preparation and catalytic performance of heterogeneous Co/PMS catalyst are affected by cobalt source, support, loading, additives, pre preparation method, calcination temperature and reaction atmosphere, but its essence is affected by the dispersion of cobalt, the reduction degree of cobalt on the surface of support, the structure and texture of support, the interaction between support and cobalt and so on. Compared with pure cobalt oxide as catalyst, the supported catalyst has more excellent properties in application: ① the catalyst complex is easy to recover and reuse and reduces the possibility of potential secondary pollution caused by the catalyst; ② Transition metals can be effectively dispersed on the surface of the loaded material, which increases the number of active sites; ③ Transition metals and load materials are connected in the form of chemical bonds, which is more stable and has a long service life. At present, the supports of heterogeneous Co / PMS system catalysts include Al<sub>2</sub>O<sub>3</sub>[139, 140], SiO<sub>2</sub>[141, 142], TiO<sub>2</sub>[143], MgO[144, 145], zeolite[146], activated carbon[147, 148][149], polytetrafluoroethylene[150], mesoporous molecular sieve, microporous molecular sieve, etc.

## 1.5 Research ideas

Efficient removal of refractory emerging pollutants in water is an important topic in the field of water environmental pollution control. With the large-scale use of antibiotics, antibiotics are widely distributed in the environment with low content, which is a potential threat to human health and ecological environment. Persulfate advanced oxidation technology based on heterogeneous catalyst has the characteristics of high efficiency, low cost and energy consumption. It is of great application value to design and develop high-efficiency new monolithic catalyst and deeply study its catalytic activation efficiency of PMS. In view of this, the main purpose of this study is to develop a new and efficient advanced sewage treatment technology, which can effectively remove the residual antibiotics in sewage. A cobalt based catalyst supported on alumina spheres with high catalytic activity was prepared and applied to persulfate advanced oxidation technology to study the removal efficiency of antibiotic pollutants; At the same time, aiming at the removal of tetracycline hydrochloride, the effects of different loading of active components and different reaction conditions on the activity of the catalyst were studied. The above research contents are of great significance for the removal of emerging pollutants in water, can provide corresponding ideas for the preparation and development of environmentally friendly functional materials, and provide theoretical basis and technical support for the removal of antibiotics in water.

## Chapter 2 Material and methods

### 2.1 Chemical reagents

All chemical reagents were used without further purification. Ferric nitrate nonahydrate ( $\text{Fe}(\text{NO}_3)_3 \cdot 9\text{H}_2\text{O}$ ,  $\geq 99.99\%$ ), Cobalt nitrate hexahydrate ( $\text{Co}(\text{NO}_3)_2 \cdot 6\text{H}_2\text{O}$ ,  $\geq 99.99\%$ ), Manganese nitrate solution ( $\text{Mn}(\text{NO}_3)_2$ , 50 wt% solution), polyvinylpyrrolidone (PVP, K29-32), Potassium peroxomonosulfate (PMS,  $\geq 42.8\%$ ), L-Histidine ( $\geq 99\%$ ), p-Benzoquinone ( $\geq 99\%$ ), 2, 4-dichlorophenol (2, 4-DCP,  $\geq 98\%$ ), 2, 4-Dichlorophenoxyacetic acid (2, 4-D,  $\geq 98\%$ ), Ciprofloxacin (CIP,  $\geq 98\%$ ), Bisphenol A (BPA,  $\geq 99\%$ ), Hydrogen peroxide solution ( $\text{H}_2\text{O}_2$ , 3 wt% in water), 5,5-Dimethylpyrroline-oxide (DMPO,  $\geq 97\%$ ), 4-Amino-2,2,6,6-tetramethylpiperidine (TEMP,  $\geq 98\%$ ) and 1, 4-benzenedicarboxylic acid ( $\text{H}_2\text{BDC}$ ,  $\geq 99\%$ ) were purchased from Aladdin Industrial Corporation. Sodium hydroxide (NaOH,  $\geq 98\%$ ), N, N-dimethyl-formamide (DMF,  $\geq 99.5\%$ ), Tert-Butyl alcohol (TBA,  $\geq 99\%$ ), ethanol ( $\geq 99.7\%$ ), Formic acid (1% w/v), Acetic acid (99.8%), HPLC grade Acetonitrile ( $\geq 99.9\%$ ) and HPLC grade methanol ( $\geq 99.9\%$ ) were purchased from Sinopharm Chemical Reagent Co. Ltd. Mung beans were purchased from a local store.

### 2.2 Synthesis of MOFs-derived LDH catalysts

CoMn-MOF was prepared by solvothermal method. 2 mmol  $\text{Mn}(\text{NO}_3)_2 \cdot 6\text{H}_2\text{O}$ , 4 mmol  $\text{Co}(\text{NO}_3)_2 \cdot 6\text{H}_2\text{O}$ , 1.2 g PVP (K29-32) and 0.6645 g  $\text{H}_2\text{BDC}$  were added in the solution containing 30 mL DMF and 20 mL ethanol, and then stirred for 1 hour at room temperature. After that, the mixture was sealed in a 100 mL Teflon-lined stainless steel autoclave and kept at  $120^\circ\text{C}$  for 24 h. After cooling to room

temperature, the product was centrifuged, then repeatedly washed with ethanol and then dried at 70°C overnight. The obtained CoMn-MOF precipitate was immersed in 50 mL 2 M NaOH aqueous solution and stirred at room temperature for 3 h to prepare CoMn-LDH. After that, the product was washed by deionized water to remove excess NaOH. Finally, the MOFs-derived LDH sample was obtained after dried at 70°C overnight. CoFe-LDH catalyst was prepared with the same methods by using 2 mmol  $\text{Fe}(\text{NO}_3)_3 \cdot 9\text{H}_2\text{O}$  instead of  $\text{Mn}(\text{NO}_3)_2 \cdot 6\text{H}_2\text{O}$ .

### **2.3 Synthesis of cobalt based Alumina pellets**

Cobalt based alumina pellets were prepared by incipient-wetness impregnation method. The detailed experimental process is as follows:

1) Determination of the quality of alumina saturated adsorbed water: the alumina pellets were washed with distilled water and ethanol respectively, then dried at 120 °C for 24 hours. 2g of dried alumina pellets were put them in a beaker, followed by dropwisely addition of distilled water until water is precipitated, and the mass M g of the dropped distilled water was calculated.

2) 2g dried alumina pellets, then weigh

A certain amount of cobalt nitrate was added into M g distilled water. After complete dissolution, cobalt nitrate solution was drop onto alumina pellets, and then dried at 100 °C for 12 hours. Then, cobalt based alumina pellet catalyst can be prepared by roasting in muffle furnace at 300 °C for 6 hours.

### **2.4 Characterization**

The X-ray diffraction (XRD) pattern of the sample was measured on a Bruker

D8 advanced X-ray powder diffractometer with Cu K $\alpha$  radiation ( $\lambda = 1.5418 \text{ \AA}$ ). The morphology and structure of LDHs were observed by using Hitachi S-4800 field emission scanning electron microscope (SEM). The transmission electron microscope (TEM) was tested by using JEOL JEM-2100 to further observe the nanostructures. The specific surface area was measured by using Micromeritics ASAP 2020 equipment to perform nitrogen adsorption-desorption measurement at 77K (Micromeritics, USA) and the sample was determined according to Brunauer-Emmett-Teller (Benselka-HadjAbdelkader et al.) analysis. Through Thermo Fisher ESCALABXi+ X-ray photoelectron spectroscopy (XPS) and Al-K (1486.6 eV) was used as the X-ray source to record then analyze the surface composition and electronic state of Co, Fe, Mg, O and other elements. The FTIR spectrum was measured at 4000-400  $\text{cm}^{-1}$  using PerkinElmer Frontier FT-IR spectrometer. Electron paramagnetic resonance (EPR, Bruker EMX/plus) was used to detect reaction species generated by the reaction through 5,5-Dimethylpyrroline-oxide (DMPO) and 4-Amino-2,2,6,6-tetramethylpiperidine (TEMP) as spin-trapping agents. The concentration of cobalt, manganese and iron were determined by the solution and used Inductively Coupled Plasma Mass Spectroscopy (ICP-MS) (Scientific iCAP RQ). The thermogravimetric analysis (TGA) and differential scanning calorimetry (DSC) were tested by METTLER TOLEDO TGA-1 thermal analyzer in a dynamic  $\text{N}_2$  atmosphere and the heating rate was  $10^\circ\text{C}/\text{min}$ .

## **2.5 Catalytic degradation experiments**

In a typical degradation experiment otherwise specified, 10 mg of catalyst (0.2 g/L) was dispersed into 50 mL of 2, 4-DCP solution (20 mg/L), and then stirred for 30

min to eliminate the effect of adsorption. After reached adsorption-desorption equilibrium, 1.0mL of PMS solution (10 mg/mL) was added into above solution to start the PMS activation reaction. After that, 1.0 mL sample was taken into a centrifuge tube every five minutes, and immediately mixed with 1.0 mL methanol to stop the catalytic reaction. Then, the collected sample was filtered through a 0.22  $\mu\text{m}$  filter membrane into an HPLC vial. Unless otherwise stated, the catalytic performance of all catalysts was evaluated in a beaker at room temperature ( $25 \pm 1^\circ\text{C}$ ), and all tests were conducted in deionized water with an initial pH ( $\text{pH}_0$ ) of 6.5. The effects of different influence factors (catalyst dosage, PMS dosage, temperature) on the PMS activation and the stability and reusability of the catalysts were also tested. In order to study the reusability of the catalyst, the catalyst was collected by centrifugation, washed several times with ethanol and deionized water and dried for the next cycle. The concentration of 2, 4-dichlorophenol and other pollutants were measured by high performance liquid chromatography (HPLC, LC-20A) equipped with Phenomenex C18 column under a UV detector and the specific test conditions for them were shown in Tab. 1. Total organic carbon (TOC) was measured by using a TOC analyzer (TOC-L, CPH, Shimadzu).

## **2.6 Phytotoxicity assessment**

The toxicity test was based on the germination rate and radicle length of mung beans (Peng et al., 2020). At the first, mung bean seeds were sterilized with 3%  $\text{H}_2\text{O}_2$ , and rinsed with ultrapure water several times. Then 100 cleaned mung beans were taken and placed on the filter paper as a carrier. The seeds were cultured by using the

undegraded 2, 4-D solution (20 mg/L), the 2, 4-DCP solution degraded by CoMn-LDH, the 2, 4-DCP solution degraded by CoFe-LDH and ultrapure water, respectively. Appropriate amount of the solution was replenished into petri dish twice a day during the culture process, respectively. And mung beans were incubated in the dark ( $25\pm 1^{\circ}\text{C}$ , 24h) for 7 days. The germination rate of mung bean seeds was recorded every 24 hours, and 20 seedlings were randomly selected from each petri dish after 7 days to count the radicle length.

**Tab.1** The analytical conditions of multiple organic pollutants

<b>Organic pollutants</b>	<b>mobile phase (v/v)</b>	<b>Flow rate (mL/min)</b>	<b>Detection wavelength (nm)</b>	<b>Reference</b>
<b>2, 4-Dichlorophenol (2, 4-DCP)</b>	Methanol/ Water = 70/30	1	283	(Wang et al., 2021)
<b>2, 4-Dichlorophenox-yacetic acid (2, 4-D)</b>	Acetonitrile/ 0.2% Formic acid = 40/60	1	284	(Li et al., 2020a)
<b>Ibuprofen (IBP)</b>	Methanol/ 0.1% Acetic acid = 60/40	1	210	(Nawaz et al., 2020)
<b>Ciprofloxacin (CIP)</b>	Acetonitrile/ 0.1% Formic acid = 20/80	1	278	(Mukherjee et al., 2021)

## Chapter 3 Characterization and catalytic performance of MOFs derived CoMn-LDH and CoFe-LDH

### 3.1 Characterization of MOFs-derived LDH catalysts

The samples obtained were initially characterized and analyzed by SEM, TEM, XRD and TG. The CoMn-LDH and CoFe-LDH samples were obtained by in-situ etching under alkaline conditions, and the hydroxyl groups were used to replace the organic ligands in MOFs. During the etching process of ligands, the crystal structures with special shapes were formed, which also created complex and hierarchical structures. As shown in Fig. 1a-b, the surface of CoMn-LDH became rough and porous, which inferred that a large number of pores were produced in the process of replacing organic ligands with hydroxyl groups. The high magnification SEM image of CoMn-LDH (Fig. 1c) further showed that there were large numbers of porous structures on the surface and arranged at layered forms. Compared to the CoMn-LDH sample, the CoFe-LDH exhibited different morphological features. The low magnification SEM images (Fig. 1d-e) manifested the formation of the porous stacked sheet structures. The high magnification image in Fig. 1e further revealed that there were irregular flake nanostructures with a width of about 500 nm on the surface.

In the XRD spectrum of CoMn-LDH (Fig. 2a), it can be seen that the peak of the crystal appeared obvious and the characteristic peaks can be matched with  $\text{Co}(\text{OH})_2$  (JCPDS: 51-1731) and  $\text{Mn}(\text{OH})_2$  (JCPDS: 18-0787). Similarly, the XRD spectrum of CoFe-LDH (Fig. 2b) peaks were obvious and the characteristic peaks of  $\text{Co}(\text{OH})_2$  (JCPDS: 74-1057) and  $\text{Fe}(\text{OH})_2$  (JCPDS: 13-0089) can be better matched. Combined with the analysis of SEM and XRD patterns, it can be concluded that the organic

ligands in MOFs were replaced by hydroxyl groups and the layered amorphous hydrotalcite-like structures were successfully synthesized, in which the reconstruction and deconstruction of the structure occurred simultaneously.

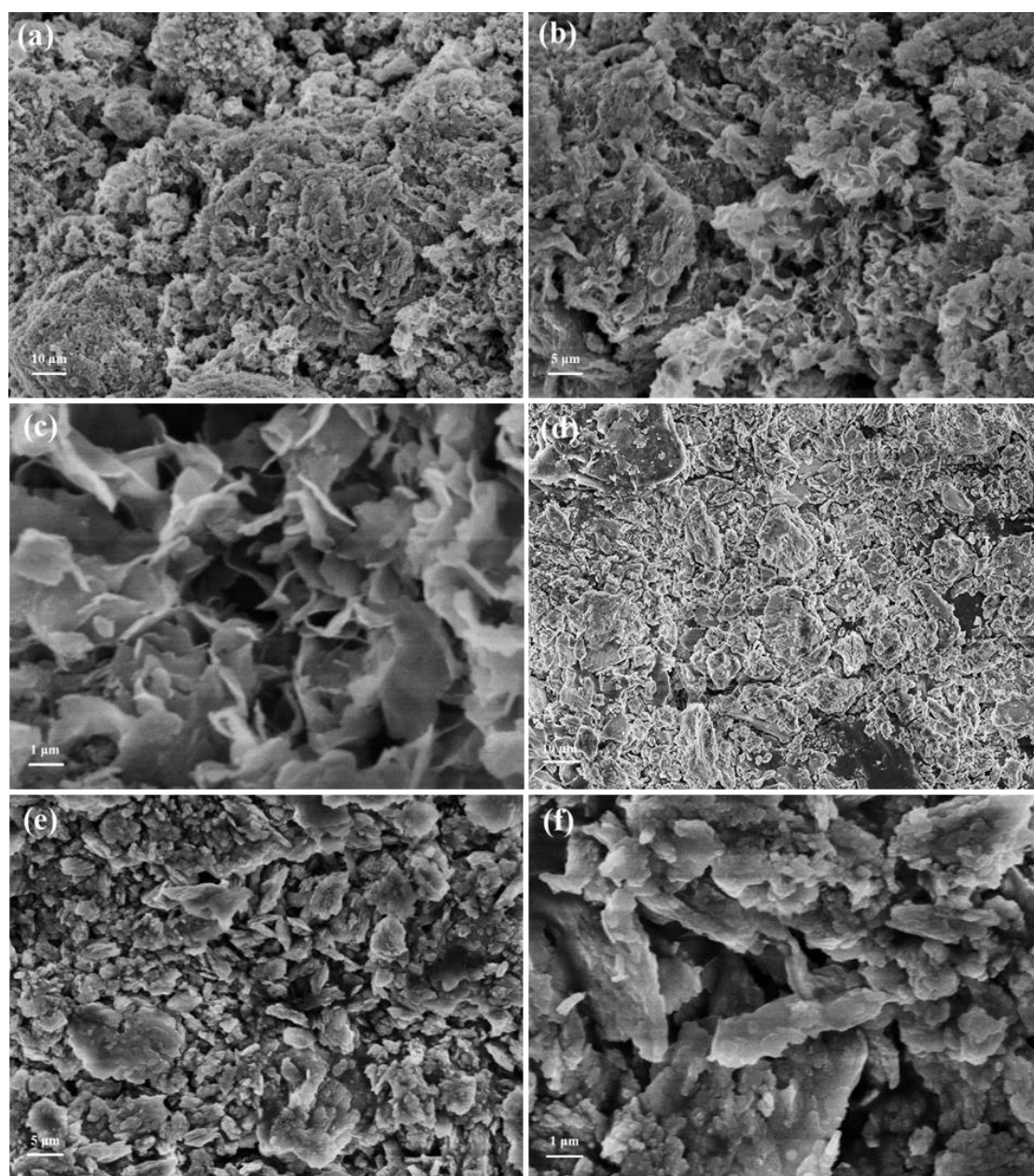


**Fig. 1.** SEM images of CoMn-LDH (a, b, c) and CoFe-LDH (d, e, f).

As shown in the FT-IR spectra (Fig. 3a), CoMn-LDH had a broad adsorption peak from 2500 to 3600  $\text{cm}^{-1}$ , which was related to the absorption of -OH group. The

characteristic peak of CoMn-LDH appeared at about  $1650\text{ cm}^{-1}$  was associated to  $-\text{COO}-$ . The bands between  $900$  and  $1500\text{ cm}^{-1}$  should be a strong absorption band of terephthalic acid ligands, but there was almost no absorption in the spectrum, which meant the organic ligands had been basically removed. Thereby, the band at  $1650\text{ cm}^{-1}$  can be attributed to the  $\text{CO}_3^{2-}$  ions existed in the LDH interlayer. For CoFe-LDH, there was a strong absorption peak at  $3631\text{ cm}^{-1}$ , which can be associated to the stretching vibration of  $-\text{OH}$ . The absorption of  $3396\text{ cm}^{-1}$  was also due to the absorption of the  $-\text{OH}$  group. The existence of the absorption peak from  $1350$  to  $1650\text{ cm}^{-1}$  indicated that the terephthalic acid ligand had been basically removed and the existence of the  $-\text{COO}-$  group. This also confirmed the presence of  $\text{CO}_3^{2-}$  ions. For CoMn-LDH and CoFe-LDH, the strong absorption around  $600\text{ cm}^{-1}$  could be attributed to the M-O and O-M-O stretching vibrations in LDHs (M = Co & Mn & Fe). The FT-IR results proved that the hydroxalite structure has been synthesized and there were inorganic anions that can be exchanged between layers and external.

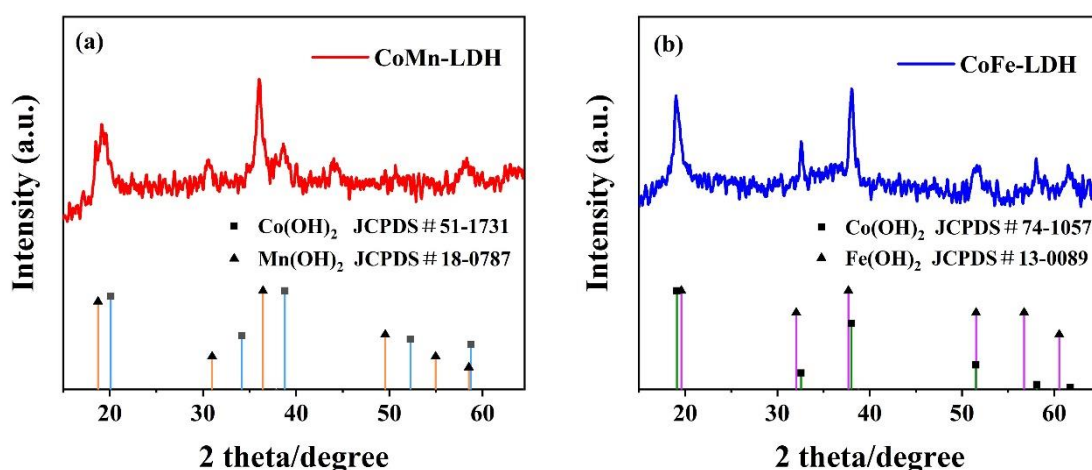


**Fig. 2.** XRD patterns of CoMn-LDH (a) and CoFe-LDH (b).

The specific surface area and pore structure of CoMn-LDH and CoFe-LDH

samples were evaluated by N<sub>2</sub> adsorption/desorption isotherm and the results were shown in Fig. 3b. The specific surface area, average pore diameter and pore volume of CoMn-LDH were 43.1 m<sup>2</sup>/g, 33.9 nm and 0.37 cm<sup>3</sup>/g, respectively. Almost all pores existed in the form of mesopores. In comparison, CoFe-LDH had a higher specific surface area of 169.9 m<sup>2</sup>/g, a smaller average pore size of 2.9 nm, and a pore volume of 0.25 cm<sup>3</sup>/g. The increased surface area of CoFe-LDH made PMS and organic pollutant molecules easier to diffuse and interact with the reaction sites, thereby increasing the reaction rate. The surface element composition and metal valence of CoMn-LDH and CoFe-LDH were obtained by X-ray photoelectron spectroscopy (XPS). As shown in Fig. 3c, the peaks of CoMn-LDH were mainly attributed to the C 1s, N 1s, O 1s, Mn 2p and Co 2p regions. The spectrum of Co 2p shown in Fig. 3d was made up of two main peaks, Co 2p<sub>3/2</sub> (779.4 eV) and Co 2p<sub>1/2</sub> (794.3 eV). The main peak with a binding energy of 779.4 eV can be decomposed into two peaks, Co<sup>3+</sup> at the peak of 779.2 eV and Co<sup>2+</sup> at the peak of 780.2 eV. As shown in Fig. 3e, the Mn 2p spectrum was composed of Mn 2p<sub>3/2</sub> (641.6 eV) and Mn 2p<sub>1/2</sub> (653.2 eV), and the two main peaks can be divided into four peaks in total. The peaks at 642.8 eV and 653.9 eV were attributed to the Mn<sup>4+</sup> species, and the peaks at 641.0 eV and 652.5 eV can be attributed to the Mn<sup>2+</sup>/Mn<sup>3+</sup> species. According to the peak area of different species, it can be found that Co<sup>3+</sup>/Co<sup>2+</sup> was 1.1, indicating that both Co<sup>3+</sup> and Co<sup>2+</sup> existed and the composition was basically the same. Meanwhile, the proportion of Mn<sup>2+</sup>/Mn<sup>3+</sup> to Mn<sup>4+</sup> was 2.1, indicating that Mn species was mainly in the form of Mn<sup>2+</sup>/Mn<sup>3+</sup>. And the atomic ratio of Mn to Co was 1:2.6. The XPS results conformed to the basic characteristics of LDH and the distribution of element valence states, and matched well with the XRD result.

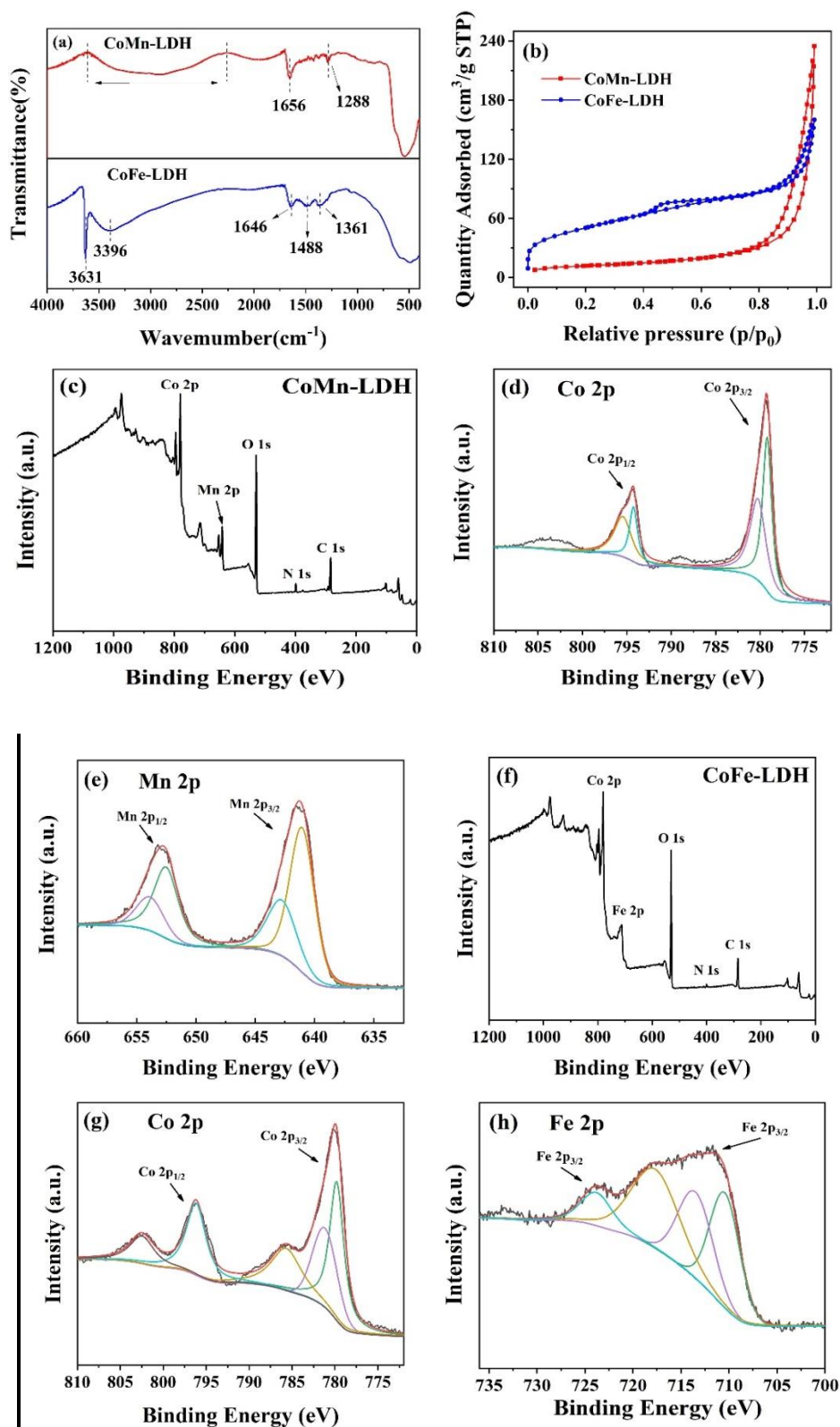


**Fig. 3.** FT-IR spectra (a) and N<sub>2</sub> adsorption-desorption isotherms (b) of CoMn-LDH and CoFe-LDH. XPS spectrum of CoMn-LDH (c) survey spectra: Co 2p (d) and Mn 2p (e); XPS spectrum of CoFe-LDH (f) survey spectra: Co 2p (g) and Fe 2p (h).

Fig. 3f showed the valence and composition of the elements in CoFe-LDH. It can be seen that the peaks were mainly composed of C 1s, N 1s, O 1s, Fe 2p and Co 2p. As shown in Fig. 3g, Co 2p mainly consisted of two main peaks and two larger satellite peaks. The main peak of Co 2p<sub>3/2</sub> at 780.2 eV can be divided into 779.8 eV and 781.2 eV. At the same time, the positions of the two satellite peak bands appear at 785.4 eV and 802.3 eV. These values matched well with the reported Co(OH)<sub>2</sub> data, which meant that the Co species in the compound presented a high-spin Co<sup>2+</sup> state, which further confirmed the existence of Co(OH)<sub>2</sub>. The XPS spectrum of Fe 2p was shown in Fig. 3h, where the Fe 2p orbital peaks were asymmetrical and there were splits and overlaps, thereby it was difficult to determine the specific composition of Fe. Generally, the appearance of satellite peaks beside the main peak meant the presence of Fe<sup>3+</sup> in the compound. Peak splitting could prove that Fe<sup>2+</sup> existed in the compound at the same time, which was consistent with formed Fe(OH)<sub>2</sub> detected by XRD results. And the atomic ratio of Fe to Co is 1:3.4. These results showed that Co<sup>2+</sup>, Fe<sup>2+</sup> and Fe<sup>3+</sup> are simultaneously present in the prepared CoFe-LDH, which also conform to the existence of hydrotalcite-like structures.

### 3.2 Catalytic performance

The following section described the 2, 4-DCP degradation via PMS activated by CoMn-LDH and CoFe-LDH catalysts under different conditions. In order to ensure the accuracy of the experimental results, each experiment was tested three times without special requirements and the average value has been taken.

After mixing of CoMn-LDH and CoFe-LDH catalysts and 2, 4-DCP solution, the 2,

4-DCP concentration of adsorption process was monitored. It could be noticed from Fig. 4a that the adsorption equilibrium reached within 15 minutes, and the adsorption rates of 2, 4-DCP by CoMn-LDH and CoFe-LDH were stable at 24.2%, 19.1%, separately. In order to eliminate the interference of adsorption on the catalytic performance, the mixture of LDH catalysts and 2, 4-DCP solution were stirred for 30 minutes before PMS addition. In addition, only 10.2% of 2, 4-DCP was degraded by PMS self-activation without addition of LDH catalysts, which indicating PMS had a weak self-activation ability to degrade pollutants.

The ability of CoMn-LDH and CoFe-LDH to adsorb dyes was weak in the absence of PMS, so catalyst adsorption effect can be excluded. In Fig. 4b, after PMS and catalyst were added simultaneously, 2, 4-DCP degradation reached 95.4% and 89.4% within 10 minutes and reached 99.3% and 99.2% within 20 minutes by CoMn-LDH and CoFe-LDH catalysts, respectively. The results showed that CoMn-LDH and CoFe-LDH exhibited excellent performance to activate PMS for 2, 4-DCP degradation.

In order to study the mineralization degree of the reaction, the TOC of the 2, 4-DCP solution was detected after 30 minutes of reaction. The removal rate of TOC reached 77.1% and 69.6% in system of CoMn-LDH/PMS and CoFe-LDH/PMS, respectively (Fig. 4c). The results indicated that the PMS activated by LDH catalysts had high removal rates of TOC, and 2, 4-DCP was degraded into small molecules and then mineralized.

During the degradation reaction, transition metals in LDH catalysts may enter the solution in the form of ions. In order to determine the degree of loss of metal ions during the catalysis process and the influence of the homogeneous catalysis of metal

ions on the experimental results, the concentration of Co ions, Mn ions and Fe ions in the reaction system were determined by ICP-MS. As shown in Fig. 4d, only 0.10 mg/L of Co ions and 0.092 mg/L Mn ions were detected in the CoMn-LDH/PMS system after 30 minutes of reaction and only 0.091 mg/L Co ions and 0.11 mg/L Fe ions were detected in the CoFe-LDH catalytic system. Such a low metal ion concentration had a negligible effect on the catalytic activity. The results proved that the MOFs-derived LDH catalysts with stable structure and excellent performance were successfully synthesized.

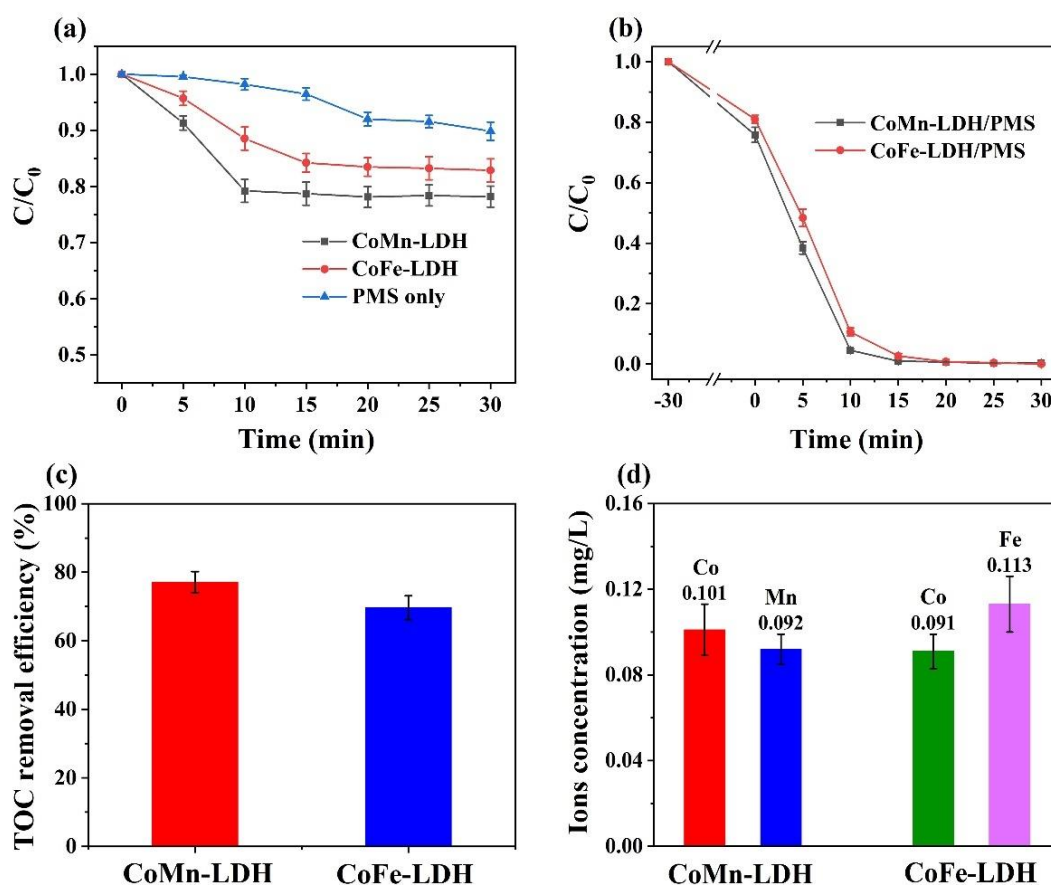
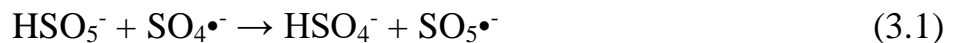


**Fig. 4.** Adsorption-desorption balance of CoMn-LDH and CoFe-LDH (a); catalytic degradation of 2, 4-DCP using different catalysts (b); TOC removal of 2, 4-DCP of CoMn LDH and CoFe-LDH (c); The concentration of cobalt ions, manganese ions

and iron ions in solution (d). The diagram is the average value of the triplicate and the error bars represent SD. Reaction conditions: [2, 4-DCP]<sub>0</sub> = 20 mg/L, [PMS]<sub>0</sub> = 0.2 g/L, [catalyst]<sub>0</sub> = 0.2 g/L, pH<sub>0</sub> = 6.5 and T<sub>0</sub> = 25°C.

### 3.3. Influence of 2, 4-DCP degradation parameters

In order to further research PMS activation performance of CoMn-LDH and CoFe-LDH, a series of 2, 4-DCP degradation experiments were carried out under different conditions (PMS concentration, catalyst dose, reaction temperature). 2, 4-DCP degradation by CoMn-LDH/PMS and CoFe-LDH/PMS at different PMS concentrations was shown in Fig. 5a-b. Obviously, as the PMS concentration increased from 0.1 g/L to 0.2 g/L (catalyst concentration: 0.2 g/L), the removal rate of 2, 4-DCP increased gradually. However, when the PMS concentration was further increased to 0.4 g/L, no significant improvement in 2, 4-DCP degradation was observed. It can be concluded that at the PMS concentration of 0.2 g/L, LDHs achieved the highest catalytic efficiency. Too high PMS concentration would produce excess reaction species, which may undergo a self-scavenging reaction, resulting in no significant improvement for 2, 4-DCP degradation. The equation represented by Eqs. (1-2).



The amount of catalyst could determine the number of active sites for PMS activation. Fig. 5c-d showed the effect of catalyst concentration on the PMS activation to degrade 2, 4-DCP. Obviously, after addition of the catalyst, the removal rate of 2, 4-DCP increased sequentially. When the amount of LDHs increased from

0.1 g/L to 0.4 g/L (PMS concentration: 0.2 g/L), 2, 4-DCP degradation by CoMn-LDH and CoFe-LDH increased from 66.9% to 77.6% and 56.2% to 78.7% within 5 minutes respectively. In fact, more catalysts provided more active sites for PMS activation, thereby further promoting the degradation of 2, 4-DCP. However, the number of catalysts only increased the initial degradation rate, but did not significantly affect the final degradation of 2, 4-DCP. The results showed 0.1 g/L catalysts could provide enough active sites to activate PMS for degrading 2,4-DCP.

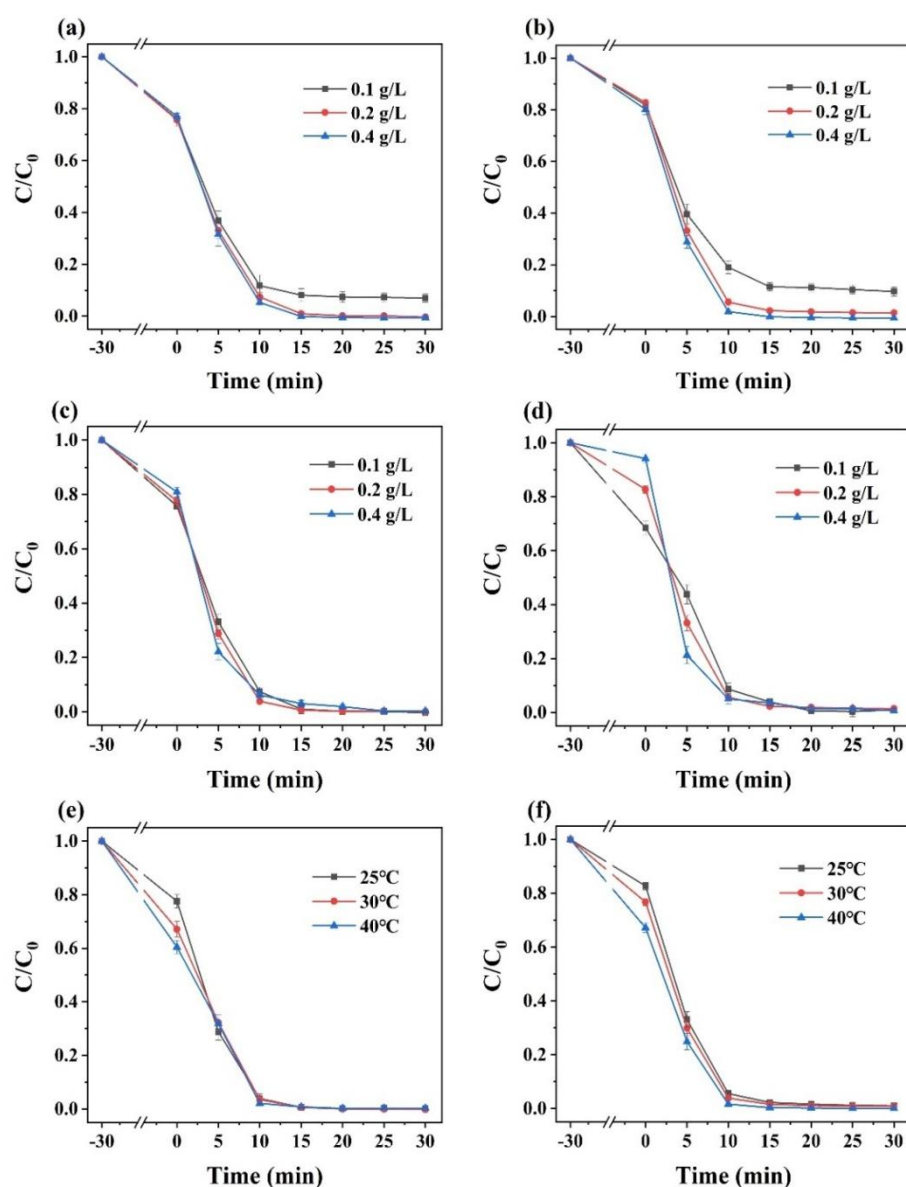


**Fig. 5.** Catalytic degradation of 2, 4-DCP under different conditions. PMS dosage

(a-b), catalyst dosage (c-d), temperature (e-f) of CoMn-LDH and CoFe-LDH, respectively. The diagram is the average value of the triplicate and the error bars represent SD. Reaction conditions:  $[2, 4\text{-DCP}]_0 = 20 \text{ mg/L}$ ,  $[\text{PMS}]_0 = 0.2 \text{ g/L}$ ,  $[\text{catalyst}]_0 = 0.2 \text{ g/L}$ ,  $\text{pH}_0 = 6.5$  and  $T_0 = 25^\circ\text{C}$ .

It can be seen from Figure 5(e) and 5(f) that when CoMn-LDH and CoFe-LDH were used as catalysts, increasing the reaction temperature can increase the degradation rate of 2, 4-DCP. In the first 10 minutes, the increase of the reaction temperature had a more obvious increase in the degradation rate, because the PMS activation is an endothermic reaction. However, after 10 minutes, the degradation rate at different temperatures tended to be the same, indicating that the temperature was not the rate determining step of the catalytic reaction.

### 3.4 Degradation test of multiple pollutants

In order to further broaden the actual application value of MOFs-derived LDHs, degradation tests of bisphenol A (BPA), ciprofloxacin (CIP) and 2,4-dichlorophenoxyacetic acid (2,4-D) were carried out (Figure 6(a) and 6(b)). In CoMn-LDH/PMS system, the degradation rates of BPA, CIP and 2,4-D reached 92.7%, 77.7% and 73.1% after 15 minutes of reaction, and 98.4%, 94.5% and 93.9% within 30 minutes, respectively. It can be seen that the pollutants have been basically removed. In CoFe-LDH/PMS system, the degradation rates of BPA, CIP and 2,4-D reached 96.8%, 93.7% and 92.3% within 30 minutes, respectively. The above results indicated that

MOFs-derived LDHs manifested excellent catalytic performance for different organic pollutant, indicating that LDHs showed great potential in environmental fields.

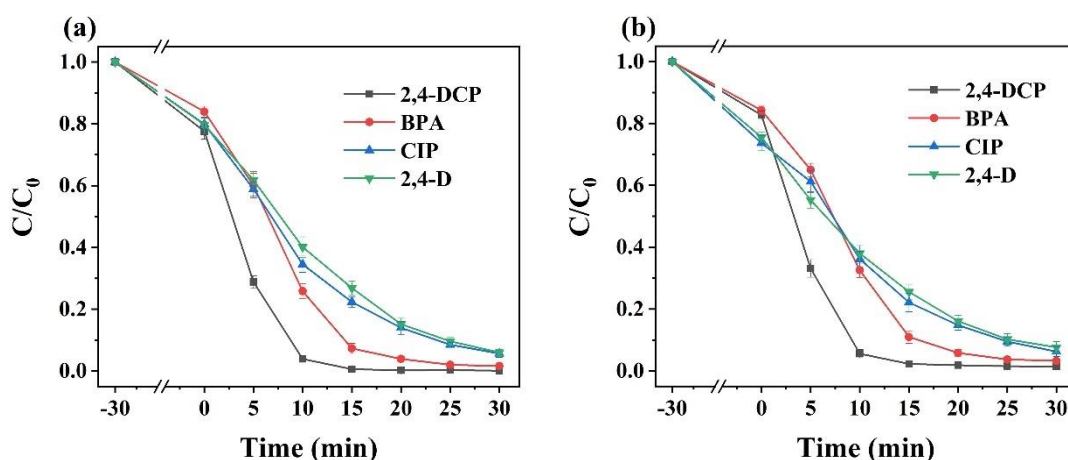


**Fig. 6.** The degradation of different pollutants by CoMn-LDH (a) and CoFe-LDH (b).

The diagram is the average value of the triplicate and the error bars represent SD.

Reaction conditions:  $[\text{pollutants}]_0 = 20 \text{ mg/L}$ ,  $[\text{PMS}]_0 = 0.2 \text{ g/L}$ ,  $[\text{catalyst}]_0 = 0.2 \text{ g/L}$ ,

$\text{pH}_0 = 6.5$  and  $T_0 = 25^\circ\text{C}$ .

### 3.5 Stability and reusability of LDHs

The reusability of the catalyst is one of the important factors to measure the stability and activity of the catalyst. Under the same reaction conditions, repeated experiments were set up to investigate the reusability of CoMn-LDH and CoFe-LDH catalysts. As shown in Figure 7(a) and 7(b), after three cycles, 2, 4-DCP degradation by CoMn-LDH and CoFe-LDH were still as high as 99.5% and 97.2%, separately. The results showed that the MOFs-derived CoMn-LDH and CoFe-LDH catalysts exhibited extremely high activity, stability and practical application value.

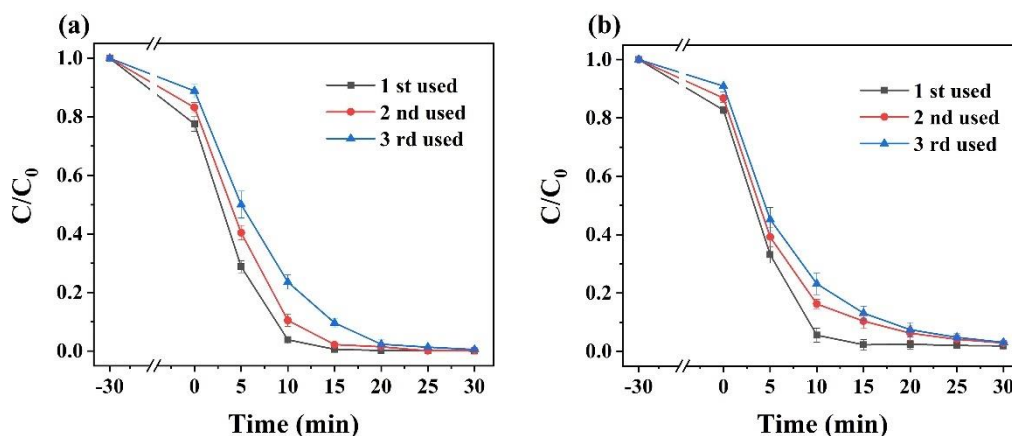


**Fig. 7.** Stability and reusability of CoMn-LDH (a) and CoFe-LDH (b) catalysts to activate PMS for 2, 4-DCP degradation. The diagram is the average value of the triplicate and the error bars represent SD. Reaction conditions:  $[2, 4\text{-DCP}]_0 = 20$  mg/L,  $[\text{PMS}]_0 = 0.2$  g/L,  $[\text{catalyst}]_0 = 0.2$  g/L,  $\text{pH}_0 = 6.5$  and  $T_0 = 25^\circ\text{C}$ .

### 3.6 Identification of reaction species and possible mechanism

MOFs-derived CoMn-LDH and CoFe-LDH catalysts showed excellent catalytic performance for PMS activation to degrade 2, 4-DCP and multiple pollutants. It is particularly important to understand the PMS activation mechanism by LDH catalysts. PMS can generate sulfate radical ( $\text{SO}_4^{\bullet-}$ ), and can also react with  $\text{H}_2\text{O}$  or  $\text{OH}^-$  to generate hydroxyl radical ( $\bullet\text{OH}$ ) (Eqs. (3-4)), which can also degrade 2, 4-DCP. Furthermore, during the PMS activation process, singlet oxygen ( $^1\text{O}_2$ ) and superoxide radicals ( $\text{O}_2^{\bullet-}$ ) may be generated to degrade 2,4-DCP. In order to determine which kind of reaction species generated in the PMS/LDH system, active reaction species quenching experiments were carried out. TBA, ethanol, L-Histidine and p-Benzoquinone were used as alternative active species scavengers to detect the existence of  $\bullet\text{OH}$ ,  $\text{SO}_4^{\bullet-}$ ,  $^1\text{O}_2$  and  $\text{O}_2^{\bullet-}$ . Ethanol can fast react with  $\bullet\text{OH}$  and  $\text{SO}_4^{\bullet-}$  to

quench free radicals. Tert-Butanol (TBA) can react quickly with  $\bullet\text{OH}$  radical, but hardly reacts with  $\text{SO}_4\bullet^-$ . In addition, the generated singlet oxygen ( $^1\text{O}_2$ ) and superoxide radicals ( $\text{O}_2\bullet^-$ ) can be scavenged by L-Histidine and p-Benzoquinone.



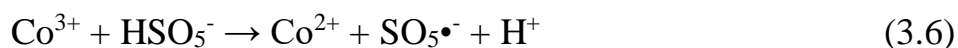
As shown in Fig. 8a-b, addition of ethanol and L-Histidine significantly reduced 2,4-DCP degradation by CoMn-LDH/PMS system and CoFe-LDH/PMS system, while the system with tert-butanol and p-Benzoquinone had relatively small reduction in the removal rate of pollutants. In the system with CoMn-LDH as the catalyst, after adding 10 mM TBA, 10 mM ethanol, 10 mM L-Histidine and 10 mM p-Benzoquinone, the removal rate of 2, 4-DCP dropped from 99.9% to 99.1%, 40.2%, 15.9% and 92.5% within 30 minutes, respectively. At the same time, in the system with CoFe-LDH as the catalyst, the removal rate of 2, 4-DCP declined from 99.1% to 97.9%, 42.9%, 34.0% and 94.6% within 30 minutes, correspondingly. In CoMn-LDH/PMS system and CoFe-LDH/PMS system with addition tert-butanol and p-Benzoquinone, 2,4-DCP was almost completely degraded within 30 minutes, but the degradation rate decreased significantly. It can be clearly seen that the inhibitory effect of L-Histidine and ethanol on 2,4-DCP removal was significantly greater than tert-butanol and p-Benzoquinone, and the inhibitory effect of L-Histidine on 2,4-DCP degradation was most obvious. Therefore, it can be concluded that  $\bullet\text{OH}$ ,  $\text{SO}_4\bullet^-$ ,  $^1\text{O}_2$  and  $\text{O}_2\bullet^-$  also can be generated by the activation of LDH catalysts, but non-radical pathways ( $^1\text{O}_2$ ) and free radical pathways ( $\text{SO}_4\bullet^-$ ) played significant roles in 2,4-DCP degradation.

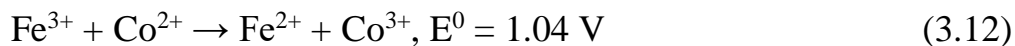
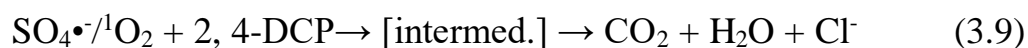
In order to further demonstrate the types of reaction species involved in the degradation reaction, electron paramagnetic resonance experiments were performed using spin-trapping agents DMPO and TEMP, which were shown in Fig. 8c-f. When only 2,4-DCP and PMS were added to the system, no signal was observed using TEMP and DMPO, which indicated that reaction species can only be produced in large quantities after catalyst activation. TEMP can be used as trapping agents for detecting  $^1\text{O}_2$  (Luo et al., 2020). When CoMn-LDH and CoFe-LDH were added to the system with TEMP as the trapping agent, a representative signal with a signal intensity ratio of 1:1:1 was detected (Fig. 8c-d), which showed that the PMS was activated and produced a large amount  $^1\text{O}_2$ . In the system with DMPO as the trapping agent, when CoMn-LDH and CoFe-LDH were added, a weak signal was detected in the CoMn-LDH system and no reaction species signal was detected in the reaction with CoFe-LDH as catalyst (Fig. 8e-f). According to the above results, both  $\text{SO}_4^{\bullet-}$  and  $^1\text{O}_2$  participated and played more important role in the PMS activation reaction, which was consistent with the results shown in Fig. 8a-b.

In order to explain the production of  $^1\text{O}_2$  and the reason why  $\text{SO}_4^{\bullet-}$  were only detected in small amounts, the production pathway of  $\text{SO}_4^{\bullet-}$  and  $^1\text{O}_2$  was further studied. Under normal circumstances,  $^1\text{O}_2$  can be slowly generated by the self-decomposition of PMS, but the production of  $^1\text{O}_2$  can be significantly promoted in the presence of carbon-based PMS activation catalysts. The C-O bond, as  $\text{sp}^2$  carbon electron rich oxides was identified as the active sites for PMS activation to generate non-radical reaction species. In addition, the presence of N atoms in CoMn-LDH and CoFe-LDH catalysts can attract the electrons of surrounding C

atoms, and the positively charged C can increase the production of  $^1\text{O}_2$  (Du et al., 2021). Meanwhile, the electron-rich N group can also provide the electrons to break the O-O bond of PMS to generate  $^1\text{O}_2$ .

Based on the above research results, a possible reaction mechanism for the catalytic activation of PMS by MOFs-derived LDH was proposed. The activation of PMS was mainly completed by the non-radical ( $^1\text{O}_2$ ) pathway and the free radical ( $\text{SO}_4^{\bullet-}$ ) pathway (Geng et al., 2021). For CoFe-LDH system, PMS reacted with  $\text{Co}^{2+}$  to generate sulfate radicals ( $\text{SO}_4^{\bullet-}$ ) and hydroxyl radicals ( $\bullet\text{HO}$ ), accompanied by one electron loss of  $\text{Co}^{2+}$  to form  $\text{Co}^{3+}$  (Eq. (5)).  $\text{Fe}^{2+}$  also lost an electron and reacted with PMS to generate  $\text{SO}_4^{\bullet-}$  and  $\bullet\text{HO}$  (Eq. (7)). The transformation between  $\text{Co}^{2+}$  and  $\text{Co}^{3+}$  can be realized through Eqs. (5-6) and  $\text{SO}_5^{\bullet-}$  can be formed at the same time. Then under the condition of MOFs-derived LDH, a large amount of  $\text{HSO}_5^-$  and  $\text{SO}_5^{\bullet-}$  were converted to  $^1\text{O}_2$  (Eq. (8)). Therefore, because a large amount of  $\text{SO}_4^{\bullet-}$  were converted into non-radical species  $^1\text{O}_2$  through the above-mentioned pathways, the number of  $\text{SO}_4^{\bullet-}$  has decreased which made it more difficult to detect. Finally, non-radicals ( $^1\text{O}_2$ ) and free radicals ( $\text{SO}_4^{\bullet-}$ ) attack the chemical bonds of 2,4-DCP to form small molecules or other intermediates, which were further mineralized into  $\text{CO}_2$ ,  $\text{H}_2\text{O}$  or  $\text{Cl}^-$  (Eq. (9)). According to the standard reduction potentials of metals (Eqs. (10-12)), it can be considered that the redox between  $\text{Co}^{2+}$  and  $\text{Fe}^{3+}$  is thermodynamically favorable.





### 3.7 Phytotoxicity assessment

2,4-D is a chlorophenoxy herbicide (CPHs), which is widely used to control the growth of various broad-leaved weeds. In order to study the toxicity of 2,4-D and its degradation intermediates, mung bean seeds were cultured in degraded 2,4-D solution for 7 days by measuring its germination rate and radicle length. It can be seen from Fig. 9a that the germination rate of mung bean seeds cultured in pure water exceeded 90% within two days, and the germination rate of mung in degraded 2,4-D solution by CoMn-LDH and CoFe-LDH decreased slightly. However, undegraded 2,4-D had a significant inhibitory effect on the germination rate of mung. Furthermore, as shown in Fig. 9b, 10-11, the average radicle length of mung bean seeds germinated in pure water, degraded 2,4-D solution (CoMn-LDH), degraded 2,4-D solution (CoFe-LDH) and undegraded 2,4-D solution were 10.3 cm, 7.4 cm, 7.0 cm and 1.1 cm. After degradation via PMS activation by LDH catalysts, the toxicity of the 2,4-D solution decreased greatly, but it still had certain inhibitory effect on the germination of mung bean, which may be due to the leakage of a small part of metal ions or the degradation of 2, 4-D intermediates affecting the growth of radicles (Kumar et al., 2021).

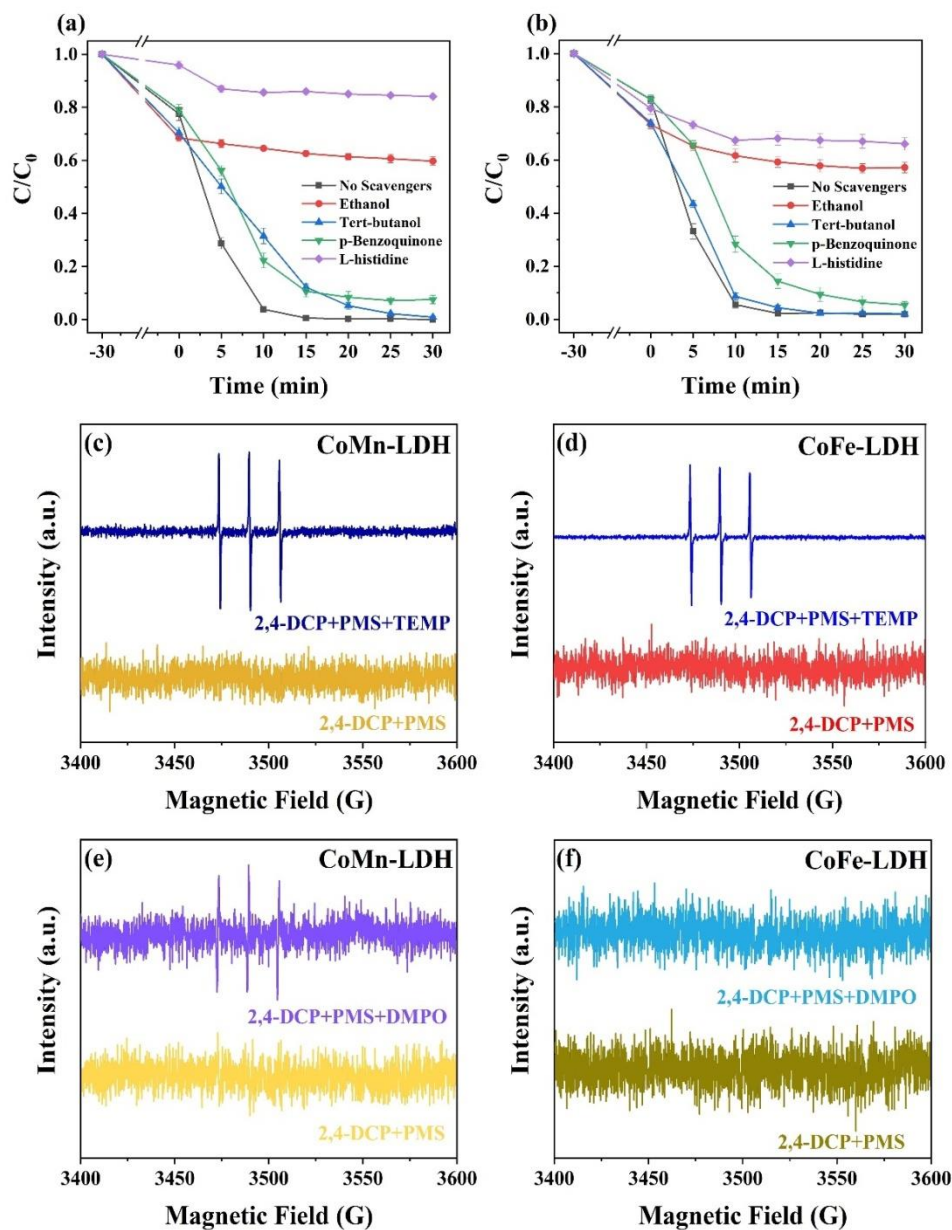


**Fig. 8.** Scavenger quenching on 2, 4-DCP degradation by ethanol, tert-Butanol, L-Histidine, p-Benzoquinone of CoMn-LDH (a) and CoFe-LDH (b); EPR spectra of CoMn-LDH catalyst in TEMP solutions (c) and in DMPO solutions (d); EPR spectra of CoFe-LDH catalyst in TEMP solutions (e) and in DMPO solutions (f). The diagram is the average value of the triplicate and the error bars represent SD. Reaction conditions:  $[2, 4\text{-DCP}]_0 = 20 \text{ mg/L}$ ,  $[\text{PMS}]_0 = 0.2 \text{ g/L}$ ,  $[\text{catalyst}]_0 = 0.2 \text{ g/L}$ ,  $\text{pH}_0 = 6.5$  and  $T_0 = 25^\circ\text{C}$ .

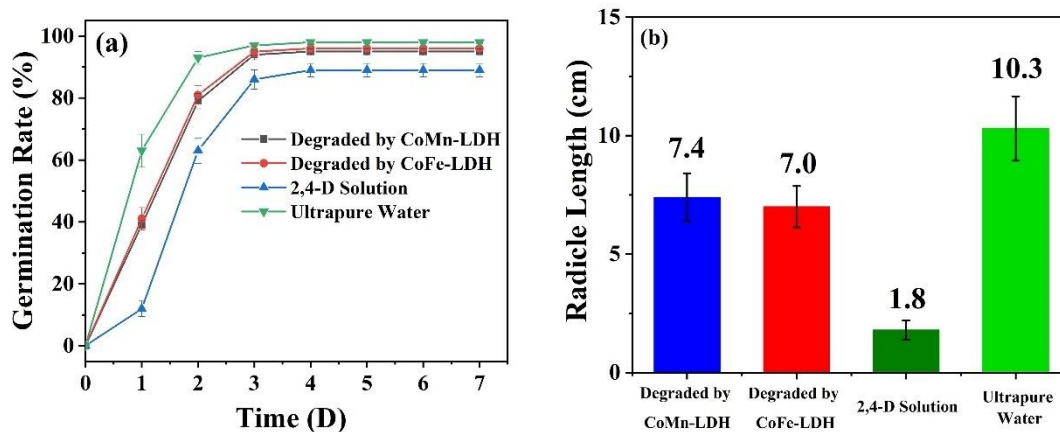


**Fig. 9.** The germination rate (a) and average radicle length (b) of mung beans cultivated in degraded 2, 4-D solution by CoMn-LDH, degraded 2, 4-D solution by CoFe-LDH, undegraded 2, 4-D solution and ultrapure water. The diagram is the average value of the triplicate and the error bars represent SD.

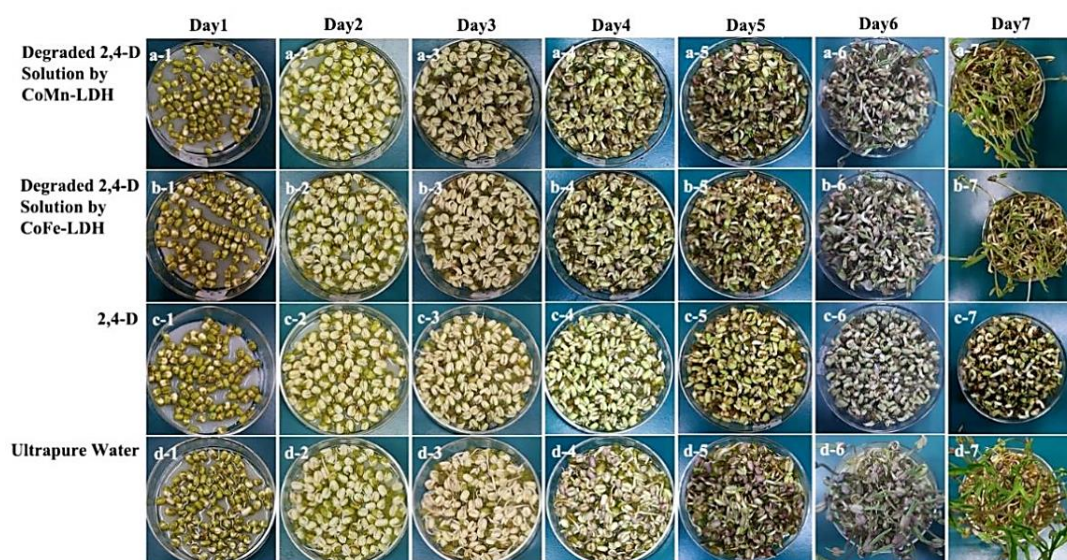


**Fig. 10.** Phytotoxicity assessment of mung beans cultivated in degraded 2,4-D solution by CoMn-LDH, degraded 2,4-D solution by CoFe-LDH, undegraded 2, 4-D solution and ultrapure water.

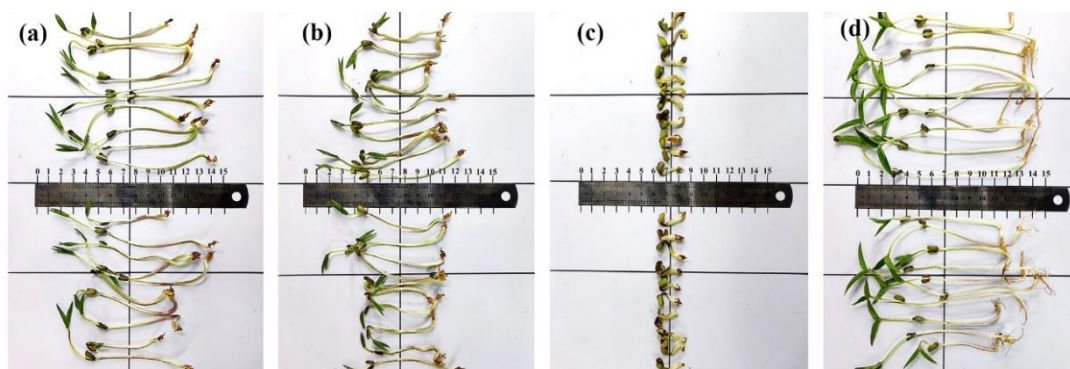


**Fig. 11.** The average radicle length of mung bean cultivated in degraded 2, 4-D solution by CoMn-LDH (a), degraded 2, 4-D solution by CoFe-LDH (b), undegraded 2, 4-D solution (c) and ultrapure water (d).

### 3.8 Conclusion

In this work, MOFs-derived CoMn-LDH and CoFe-LDH catalysts with high activity and high specific surface area were successfully prepared through the pseudomorphic transformation process under alkaline conditions. The SEM and TEM manifested that the two LDH catalysts have a stable layered structure, and the morphology basically did not change even after use. BET results showed that two LDHs have well-developed porous structures and high specific surface area, which could provide more active site to activate PMS. As a result, the two LDH samples demonstrated high catalytic performance to activate PMS for the degradation of 2, 4-DCP and other organic pollutant. 2, 4-DCP degradation by CoMn-LDH/PMS system and CoFe-LDH/PMS system reached 99.3% and 99.2% within 20 minutes, respectively. The moderate increase of PMS concentration, catalyst dosage and reaction temperature all have a positive effect on the degradation of 2, 4-DCP. After three cycles, CoMn-LDH and CoFe-LDH catalysts could still obtain 2, 4-DCP degradation of 99.5% and 97.2%, indicating that MOFs derived LDH catalysts are

stable and excellent candidates for PMS activation. In addition, these two LDH catalysts also showed excellent catalytic performance for the degradation of other different types of pollutants, such as BPA, CIP, 2, 4-D. The high activity of the two LDH catalysts was attributed to the large specific surface area, hierarchical structure, redox reaction. The scavenger experiments and EPR results showed that  $^{\bullet}O_2$  and  $SO_4^{\bullet-}$  were the main active substance in 2, 4-DCP degradation. In addition, phytotoxicity assessment of mung beans confirmed the significant enhancement in mineralization degree and reduction toxicity of the degraded 2, 4-D solution by two LDH catalysts. In summary, this research provided a facile method to design transition metal based LDH samples and expands the scope of MOFs derivants for PMS activation in organic wastewater treatment.

## Chapter 4 Catalytic performance of cobalt based Alumina pellets

The LDH catalyst derived from MOFs showed high activity in activating PMS to degrade different pollutants, but the LDH catalysts are still powder catalyst. After the degradation reaction, the catalyst needs to be separated by filtration or centrifugation, which increases the operation cost. The problem of subsequent separation of catalyst can be solved by using monolithic support to load active components. At present, the researchers used graphene aerogels or foam metal carriers to load active components to activate PMS to degrade pollutants. Yuan et al. [151] added the prepared cobalt oxide nanoparticles into the precursor solution of graphene. After hydrothermal treatment, three dimensional  $\text{Co}_3\text{O}_4$ /nitrogen doped graphene aerogels ( $\text{Co}_3\text{O}_4$ /NGA) were prepared by freeze drying. (as shown in Fig. 12), the synergistic effect between  $\text{Co}_3\text{O}_4$  nanocrystals and new active sites formed by three-dimensional structure of nitrogen doped graphene has high catalytic activity.  $\text{Co}_3\text{O}_4$ /NGA catalyst realizes the complete degradation of acid orange within 30min, shows high stability in the cycle experiment, and the subsequent separation is simple. Zhang et al. [152] prepared graphene with high mechanical strength and high elasticity by mixing graphene with cobalt nitrate and methylamine, hydrothermal, freeze-drying and roasting  $\text{CoO}@GA$ , the catalyst showed high chloramphenicol degradation activity in 9 cycles. Peng and other [153] were prepared by in-situ growth of ZIF-67 on foamed nickel to form an integrated NF/ZIF-67 catalyst. In the degradation experiment of Rhodamine B (Rh b), more than 99% of Rh B was degraded within half an hour, but after four cycle experiments, the degradation rate of the catalyst decreased to 90%. Yuan [154] prepared nickel foam supported  $\text{Co}_3\text{O}_4$ /NF

catalyst by hydrothermal method. The decolorization of Acid Orange 7 could be achieved in 30min. After 10 cycles, the catalyst remained highly active and the leakage of cobalt ions was only 11-23  $\mu\text{g/L}$ , which is far lower than the maximum allowable concentration of drinking water and natural water (100  $\mu\text{g/L}$ ).

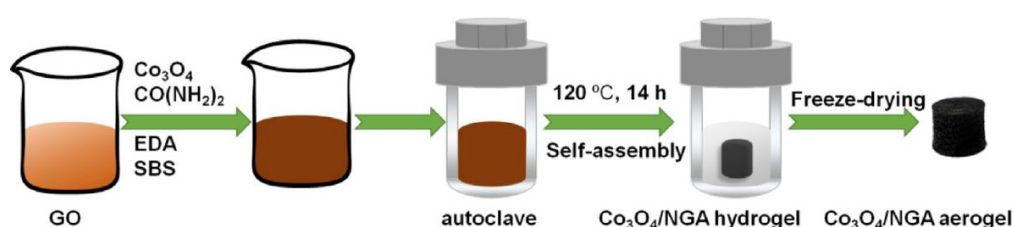


**Fig. 12. Schematic diagram for the synthesis of  $\text{Co}_3\text{O}_4/\text{NGA}$  catalyst[151]**

Alumina pellets are particles with many capillary channels and have strong affinity for substances with strong polarity of water molecules. They are a non-toxic and non corrosive high-efficiency adsorbent with the characteristics of high static capacity, low grinding consumption, no fear of water and strong absorption capacity. At present, alumina spheres are widely used in the field of catalysis. In this study, alumina spheres were used as a carrier to support cobalt for activating PMS to degrade tetracycline hydrochloride.

Alumina pellets are particles with many capillary channels and have strong affinity for substances with strong polarity of water molecules. They are a non-toxic and non corrosive high-efficiency adsorbent with the characteristics of high static capacity, low grinding consumption, no fear of water and strong absorption capacity. At present, alumina spheres are widely used in the field of catalysis. In this study, alumina spheres were used as a carrier to support cobalt for activating PMS to degrade tetracycline hydrochloride.

## 4.1 Results and discussion

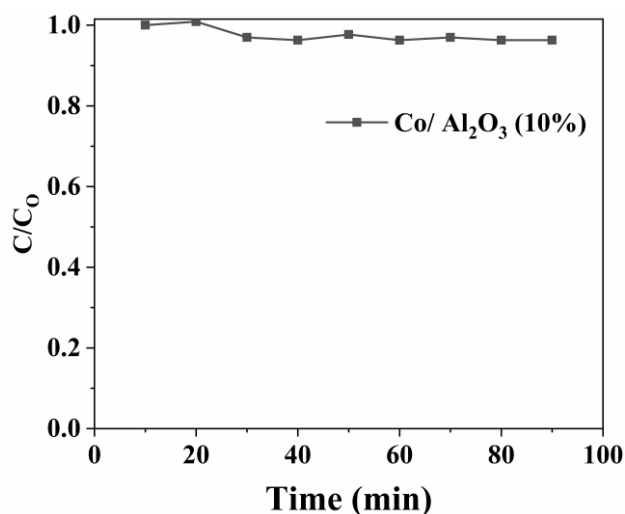


**Fig. 13.** Catalytic adsorption of TC of Co/Al<sub>2</sub>O<sub>3</sub> (10 %)

Reaction conditions: [TC]<sub>0</sub> = 100 mg·L<sup>-1</sup>, [catalyst]<sub>0</sub> = 1 g·L<sup>-1</sup>, pH = 7.0, and T = 25 °C

Fig. 13 shows the adsorption performance of Co/Al<sub>2</sub>O<sub>3</sub> catalyst on tetracycline hydrochloride (100 mg/L). The data showed that the adsorption capacity of Co/Al<sub>2</sub>O<sub>3</sub> catalyst was weak, and only 4% tetracycline hydrochloride was adsorbed after 90 minutes. This may be due to the small specific surface area of the Co/Al<sub>2</sub>O<sub>3</sub> catalyst itself or the high concentration of tetracycline hydrochloride. Therefore, the concentration of tetracycline hydrochloride was adjusted to 30mg/L to further explore the experiment.

Figure 14 shows the adsorption effect of Co/Al<sub>2</sub>O<sub>3</sub> catalyst on tetracycline hydrochloride (30 mg/L). The data show that the adsorption capacity of the Co/Al<sub>2</sub>O<sub>3</sub> catalyst is still weak when the concentration of tetracycline hydrochloride is 30 mg/L. At 90 minutes, only 7% tetracycline hydrochloride was adsorbed. Therefore, it can be preliminarily judged that the low adsorption amount is due to the small specific

surface area of the catalyst.

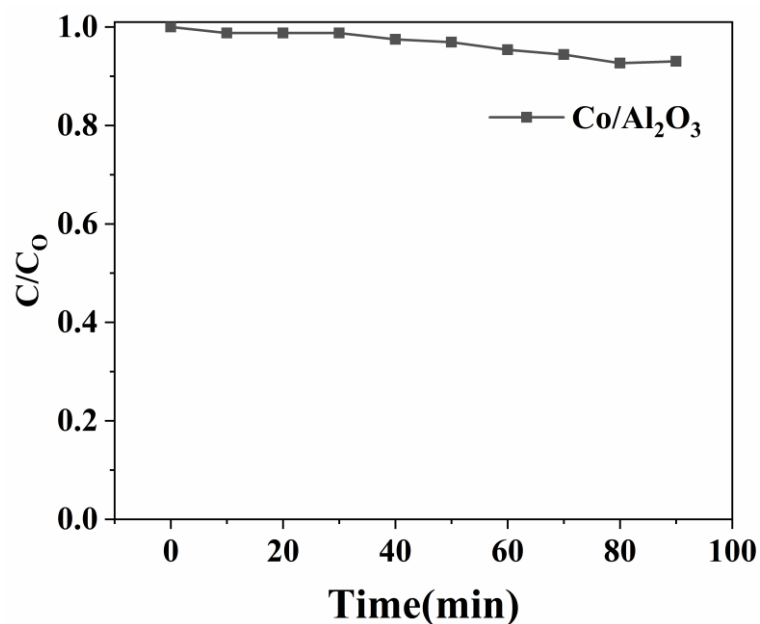


**Fig. 14.** Catalytic adsorption of TC of Co /Al<sub>2</sub>O<sub>3</sub> (10 %)

Reaction conditions: [TC]<sub>0</sub> = 30 mg·L<sup>-1</sup>, [catalyst]<sub>0</sub> = 1 g·L<sup>-1</sup>, pH = 7.0, and T = 25 °C

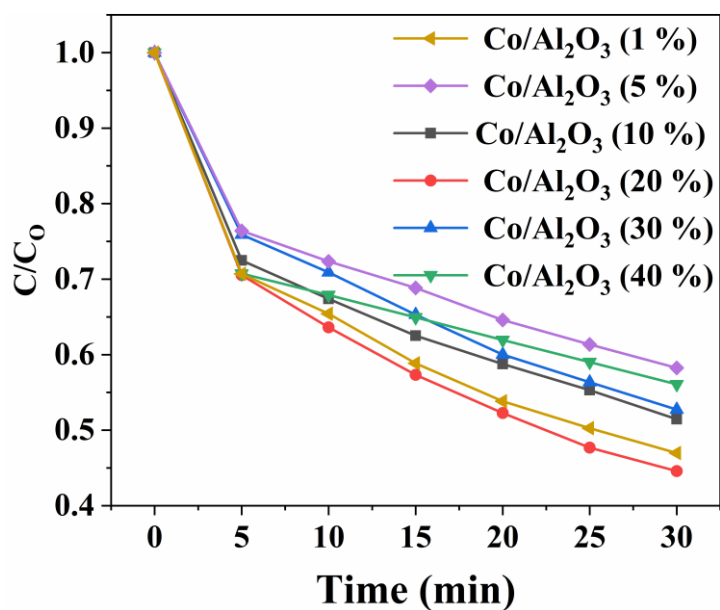


**Fig. 15.** Catalytic degradation of TC using catalysts with different loads.

Reaction conditions: [TC]<sub>0</sub> = 30 mg·L<sup>-1</sup>, [PMS]<sub>0</sub> = 0.1 g/L, [catalyst]<sub>0</sub> = 1 g·L<sup>-1</sup>, pH = 7.0, and T = 25 °C

Fig. 15 shows the degradation of tetracycline hydrochloride (30 mg/L) with different loading amounts of Co/Al<sub>2</sub>O<sub>3</sub> catalyst. The data showed that after 30 minutes of reaction, the degradation rates of tetracycline hydrochloride catalyzed by PMS activated by Co/Al<sub>2</sub>O<sub>3</sub>(1%), Co/Al<sub>2</sub>O<sub>3</sub>(5%), Co/Al<sub>2</sub>O<sub>3</sub>(10%), Co/Al<sub>2</sub>O<sub>3</sub>(20%), Co/Al<sub>2</sub>O<sub>3</sub>(30%) and Co/Al<sub>2</sub>O<sub>3</sub>(40%) catalysts were 54%, 42%, 49%, 56%, 48% and 44%, respectively. It can be seen that the activity of the catalyst is higher when the loading amount of cobalt is 1% and 20%. Among them, when the loading amount is 20%, the degradation effect of TC reaches the best. With the increase of loading amount Co, the degradation effect no longer shows an upward trend. This shows that Al<sub>2</sub>O<sub>3</sub> as a carrier has limited load effect. This may be due to the optimal number of active sites provided by 20% Co load when PMS is added. It is very important to find a catalyst with high efficiency and appropriate ratio.

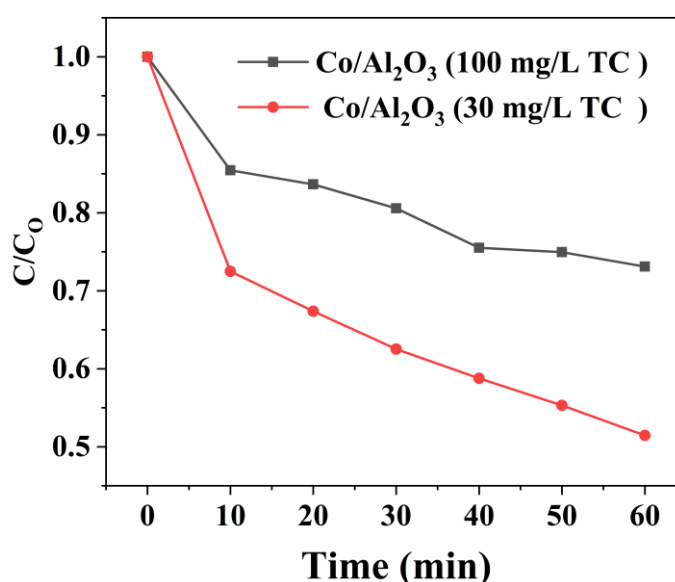


**Fig. 16.**Effect of TC concentration on TC degradation in Co/Al<sub>2</sub>O<sub>3</sub>/PMS system.

Reaction conditions: [PMS]<sub>0</sub> = 0.1 g/L, [catalyst]<sub>0</sub> = 1 g·L<sup>-1</sup>, pH = 7.0, and T = 25 °C

Figure 16 shows the degradation effect of Co/Al<sub>2</sub>O<sub>3</sub> (10%) catalyst on tetracycline hydrochloride of 30 mg/L and 100 mg/L. The data show that the degradation efficiency of Co/Al<sub>2</sub>O<sub>3</sub> (10%) for tetracycline hydrochloride of 30 mg/L reaches 49%. When the concentration of pollutant TC is 100 mg/L, the degradation rate is only 23%, which indicates that the degradation efficiency decreases significantly with the increase of the concentration of pollutant TC. This may be due to the limited active sites provided by Co/Al<sub>2</sub>O<sub>3</sub> catalyst at the same time. Therefore, the ability to attack the functional groups of organic compounds is limited and the degradation effect is not ideal.

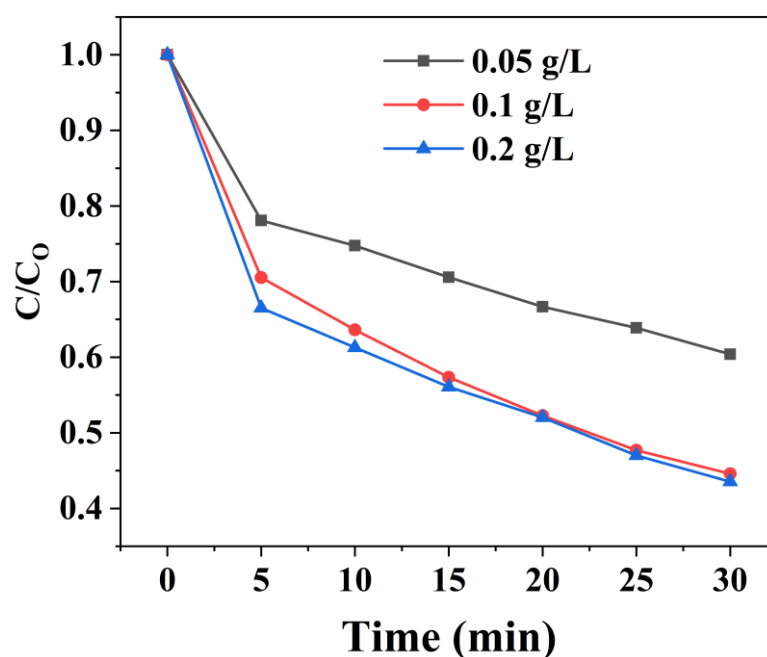


**Fig. 17.**Effect of PMS concentration on TC degradation in Co/Al<sub>2</sub>O<sub>3</sub>/PMS system

Reaction conditions: [TC]<sub>0</sub> = 30 mg·L<sup>-1</sup>, [PMS]<sub>0</sub> = 0.1 g/L, [catalyst]<sub>0</sub> = 1 g·L<sup>-1</sup>, pH = 7.0, and T = 25 °C

Fig. 17 shows the degradation effect of Co/Al<sub>2</sub>O<sub>3</sub> catalyst on PMS with concentrations of 0.05 g/L, 0.1 g/L and 0.2 g/L. With the increase of PMS

concentration in the reaction system, the degradation rate of tetracycline hydrochloride increased gradually. When the concentration of PMS in the reaction system increased to 0.2 g/L, 58% of TC could be removed within 30 minutes. The reason for this phenomenon may be that with the increase of PMS concentration, more and more oxidative active species are activated, and there is a large amount of  $\text{SO}_4^{\bullet-}$  in the reaction system to degrade tetracycline hydrochloride. However, with the increase of PMS concentration, the degradation efficiency does not increase significantly, which may be caused by the saturation of the active site of the catalyst itself in the reaction system.

## 4.2 Conclusion

In conclusion, a series of low-cost transition metal supported alumina pellet catalysts were prepared by simple impregnation method with cobalt nitrate as precursor. With the gradual increase of cobalt loading, the activity of catalyst activated PMS for the degradation of tetracycline hydrochloride continues to increase, but when the loading continues to increase, the activity of the catalyst begins to decline, and the optimal cobalt loading is 20wt%.  $\text{Co}/\text{Al}_2\text{O}_3(20\%)$  catalyst can remove 55% tetracycline hydrochloride within 30 minutes. At the same time, different PMS concentrations also have a great impact on the degradation activity of the catalyst, and the optimal addition of PMS is 0.1mg/l

## Conclusion and research prospect

### 5.1 Conclusions

In this paper, MOFs derived LDH catalysts were prepared by hydrothermal method and alkali etching method. Cobalt based alumina microsphere catalysts were synthesized by simple impregnation method. The research fields mainly include the degradation of chlorophenols, including the study of their activation mechanism. The physicochemical properties of the catalyst were analyzed by a series of characterization methods such as XRD, BET, XPS, SEM and EPR. The obtained catalyst was used to activate PMS to catalyze the degradation of 2,4-DCP and other organic pollutants in water, such as pesticides and antibiotics. The effects of different reaction conditions in the reaction system on the catalytic degradation effect and the specific degradation mechanism of 2,4-DCP were explored. The research of this paper mainly includes the following three aspects:

(1) MOFs were prepared by a simple hydrothermal method. As a precursor, CoMn LDH and CoFe LDH catalysts with high specific surface area perovskite catalysts were obtained by etching in alkaline solution. The obtained LDH catalyst has a sheet structure, indicating the formation of a layered structure. CoMn LDH and CoFe LDH catalysts have large specific surface area and significantly improve the degradation efficiency of organic pollutants. Through the results of PMS degradation activated by CoMn LDH and CoFe LDH, it can be seen that both CoMn LDH and CoFe LDH have high PMS activation properties.

(2) Cobalt based alumina microsphere catalysts were prepared by a simple impregnation method. The carrier of the catalyst is alumina microspheres. With very

little loading of cobalt nanoparticles, it can achieve efficient PMS activation and degradation effect, which greatly reduces the cost of activated PMS degradation of organic pollutants. At the same time, when the loading amount of cobalt is 20%, the activity of the catalyst is the highest. At the same time, when the addition amount of PMS is 0.1g/l, the activity of the catalyst is the highest. The catalyst has strong mechanical properties and stability, can be recycled for many times, and can avoid the problems of secondary pollution and difficult recovery caused by the catalytic process.

## **5.2 Research prospect**

The research of this paper can also be improved from the following aspects:

(1) At present, the catalytic degradation of advanced oxidation technology is mainly in the basic research. Because of its advantages, it has good application value and prospect in practical industrial application. What we want to improve is to make the cobalt based alumina catalyst into the filler in the fixed bed, the sewage flows in from one side and the treated water flows out from the other side, so as to quickly achieve the purpose of rapid sewage treatment, improve the industrial application value of the integral catalyst and make some contributions to water treatment.

(2) In order to make rational use of existing resources, we introduce photocatalysis into the process of activating PMS to degrade chlorophenols organic pollutants, so as to effectively use light energy and reduce the utilization of oxidants, which can not only reduce the cost of sewage treatment, but also maximize the utilization of resources.

## Reference

- [1] A.S. Ezeuko, M.O. Ojemaye, O.O. Okoh, A.I. Okoh, Technological advancement for eliminating antibiotic resistance genes from wastewater: A review of their mechanisms and progress, *Journal of Environmental Chemical Engineering*, 9 (2021).
- [2] X. Liu, X. Guo, Y. Liu, S. Lu, B. Xi, J. Zhang, Z. Wang, B. Bi, A review on removing antibiotics and antibiotic resistance genes from wastewater by constructed wetlands: Performance and microbial response, *Environmental Pollution*, 254 (2019).
- [3] C. Uluseker, K.M. Kaster, K. Thorsen, D. Basiry, S. Shobana, M. Jain, G. Kumar, R. Kommedal, I. Pala-Ozkok, A Review on Occurrence and Spread of Antibiotic Resistance in Wastewaters and in Wastewater Treatment Plants: Mechanisms and Perspectives, *Frontiers in microbiology*, 12 (2021) 717809-717809.
- [4] S. Mallakpour, E. Azadi, Nanofiltration membranes for food and pharmaceutical industries, *Emergent Materials*, (2021).
- [5] R. Xu, W. Qin, B. Zhang, X. Wang, T. Li, Y. Zhang, X. Wen, Nanofiltration in pilot scale for wastewater reclamation: Long-term performance and membrane biofouling characteristics, *Chemical Engineering Journal*, 395 (2020).
- [6] K. Slipko, D. Reif, M. Woegerbauer, P. Hufnagl, J. Krampe, N. Kreuzinger, Removal of extracellular free DNA and antibiotic resistance genes from water and wastewater by membranes ranging from microfiltration to reverse osmosis, *Water Research*, 164 (2019).
- [7] Q. Xiang, Y. Nomura, S. Fukahori, T. Mizuno, H. Tanaka, T. Fujiwara, Innovative Treatment of Organic Contaminants in Reverse Osmosis Concentrate from Water Reuse: a Mini Review, *Current Pollution Reports*, 5 (2019) 294-307.

- [8] Y. Zong, S. Ma, J. Gao, M. Xu, J. Xue, M. Wang, Synthesis of Porphyrin Zr-MOFs for the Adsorption and Photodegradation of Antibiotics under Visible Light, *Acs Omega*, 6 (2021) 17228-17238.
- [9] S.-H. Liu, C.-C. Lu, C.-W. Lin, S.-H. Chang, Rapid modification of waste expanded polystyrene with H<sub>2</sub>SO<sub>4</sub>/trace persulfate in one pot for effective adsorption of fluoroquinolone antibiotic and its regeneration, *Chemosphere*, 271 (2021).
- [10] L.R.d.C. Costa, L.A. Feris, Use of functionalized adsorbents for tetracycline removal in wastewater: adsorption mechanism and comparison with activated carbon, *Journal of Environmental Science and Health Part a-Toxic/Hazardous Substances & Environmental Engineering*, 55 (2020) 1604-1614.
- [11] I. Kariim, A.S. Abdulkareem, O.K. Abubakre, Development and characterization of MWCNTs from activated carbon as adsorbent for metronidazole and levofloxacin sorption from pharmaceutical wastewater: Kinetics, isotherms and thermodynamic studies, *Scientific African*, 7 (2020).
- [12] F. Yin, S. Lin, X. Zhou, H. Dong, Y. Zhan, Fate of antibiotics during membrane separation followed by physical-chemical treatment processes, *Science of the Total Environment*, 759 (2021).
- [13] P.Y. Nguyen, G. Carvalho, M.A.M. Reis, A. Oehmen, A review of the biotransformations of priority pharmaceuticals in biological wastewater treatment processes, *Water Research*, 188 (2021).
- [14] B. Li, F. Jing, D. Wu, B. Xiao, Z. Hu, Simultaneous removal of nitrogen and phosphorus by a novel aerobic denitrifying phosphorus-accumulating bacterium, *Pseudomonas stutzeri* ADP-19, *Bioresource Technology*, 321 (2021).

- [15] R. Xu, Y. Zhang, W. Xiong, W. Sun, Q. Fan, Z. Yang, Metagenomic approach reveals the fate of antibiotic resistance genes in a temperature-raising anaerobic digester treating municipal sewage sludge, *Journal of Cleaner Production*, 277 (2020).
- [16] H. Tikariha, H.J. Purohit, Unfolding microbial community intelligence in aerobic and anaerobic biodegradation processes using metagenomics, *Archives of Microbiology*, 202 (2020) 1269-1274.
- [17] A.a. Gobel, A. Thomsen, C.S. McArdell, A.C. Alder, W. Giger, N. Theiss, D. Löffler, T.A. Ternes, Extraction and determination of sulfonamides, macrolides, and trimethoprim in sewage sludge, *Journal of chromatography. A*, 1085 (2005) 179-189.
- [18] L. Zhou, F. Lv, L. Liu, S. Wang, Water-Soluble Conjugated Organic Molecules as Optical and Electrochemical Materials for Interdisciplinary Biological Applications, *Accounts of Chemical Research*, 52 (2019) 3211-3222.
- [19] J.F. de Carvalho, J.E.F. de Moraes, Treatment of simulated industrial pharmaceutical wastewater containing amoxicillin antibiotic via advanced oxidation processes, *Environmental Technology*, 42 (2021) 4145-4157.
- [20] L. Liu, Z. Chen, J. Zhang, D. Shan, Y. Wu, L. Bai, B. Wang, Treatment of industrial dye wastewater and pharmaceutical residue wastewater by advanced oxidation processes and its combination with nanocatalysts: A review, *Journal of Water Process Engineering*, 42 (2021).
- [21] M. Verma, A.K. Haritash, Review of advanced oxidation processes (AOPs) for treatment of pharmaceutical wastewater, *Advances in Environmental Research-an International Journal*, 9 (2020) 1-17.

- [22] J. Wang, R. Zhuan, Degradation of antibiotics by advanced oxidation processes: An overview, *Science of the Total Environment*, 701 (2020).
- [23] I. Grcic, D. Vujevic, J. Sepcic, N. Koprivanac, Minimization of organic content in simulated industrial wastewater by Fenton type processes: A case study, *Journal of Hazardous Materials*, 170 (2009) 954-961.
- [24] J. Carbajo, J.E. Silveira, G. Pliego, J.A. Zazo, J.A. Casas, Increasing Photo-Fenton process Efficiency: The effect of high temperatures, *Separation and Purification Technology*, 271 (2021).
- [25] S. Giannakis, K.-Y.A. Lin, F. Ghanbari, A review of the recent advances on the treatment of industrial wastewaters by Sulfate Radical-based Advanced Oxidation Processes (SR-AOPs), *CHEMICAL ENGINEERING JOURNAL*, 406 (2021).
- [26] J. Peng, Y. He, C. Zhou, S. Su, B. Lai, The carbon nanotubes-based materials and their applications for organic pollutant removal: A critical review, *CHINESE CHEMICAL LETTERS*, 32 (2021) 1626-1636.
- [27] M. Lapertot, S. Ebrahimi, S. Dazio, A. Rubinelli, C. Pulgarin, Photo-Fenton and biological integrated process for degradation of a mixture of pesticides, *Journal of Photochemistry and Photobiology A: Chemistry*, 186 (2007) 34-40.
- [28] J. Monteagudo, A. Durán, I. San Martin, M. Aguirre, Catalytic degradation of Orange II in a ferrioxalate-assisted photo-Fenton process using a combined UV-A/C–solar pilot-plant system, *Applied Catalysis B: Environmental*, 95 (2010) 120-129.
- [29] Y. Yang, P. Wang, S. Shi, Y. Liu, Microwave enhanced Fenton-like process for the treatment of high concentration pharmaceutical wastewater, *Journal of Hazardous*

Materials, 168 (2009) 238-245.

[30] C.-H. Weng, Y.-T. Lin, C.-K. Chang, N. Liu, Decolourization of direct blue 15 by Fenton/ultrasonic process using a zero-valent iron aggregate catalyst, Ultrasonics sonochemistry, 20 (2013) 970-977.

[31] P. Gao, Y. Song, M. Hao, A. Zhu, H. Yang, S. Yang, An effective and magnetic Fe<sub>2</sub>O<sub>3</sub>-ZrO<sub>2</sub> catalyst for phenol degradation under neutral pH in the heterogeneous Fenton-like reaction, Separation and Purification Technology, 201 (2018) 238-243.

[32] N. Wang, L. Zhu, D. Wang, M. Wang, Z. Lin, H. Tang, Sono-assisted preparation of highly-efficient peroxidase-like Fe<sub>3</sub>O<sub>4</sub> magnetic nanoparticles for catalytic removal of organic pollutants with H<sub>2</sub>O<sub>2</sub>, Ultrasonics Sonochemistry, 17 (2010) 526-533.

[33] N. Wang, L. Zhu, M. Wang, D. Wang, H. Tang, Sono-enhanced degradation of dye pollutants with the use of H<sub>2</sub>O<sub>2</sub> activated by Fe<sub>3</sub>O<sub>4</sub> magnetic nanoparticles as peroxidase mimetic, Ultrasonics sonochemistry, 17 (2010) 78-83.

[34] L. Xu, J. Wang, A heterogeneous Fenton-like system with nanoparticulate zero-valent iron for removal of 4-chloro-3-methyl phenol, Journal of hazardous materials, 186 (2011) 256-264.

[35] Y. Tian, X. Tian, W. Zeng, Y. Nie, C. Yang, C. Dai, Y. Li, L. Lu, Enhanced peroxymonosulfate decomposition into  $\cdot$ OH and  $^{1}O_2$  for sulfamethoxazole degradation over Se doped g-C<sub>3</sub>N<sub>4</sub> due to induced exfoliation and N vacancies formation, SEPARATION AND PURIFICATION TECHNOLOGY, 267 (2021).

[36] K.-L. Shao, Z.-X. Ye, H. Huang, X. Yang, ClO<sub>2</sub> pre-oxidation impacts the formation and nitrogen origins of dichloroacetonitrile and dichloroacetamide during

subsequent chloramination, *Water Research*, 186 (2020).

[37] N. Augsburger, N. Zaouri, H. Cheng, P.-Y. Hong, The use of UV/H<sub>2</sub>O<sub>2</sub> to facilitate removal of emerging contaminants in anaerobic membrane bioreactor effluents, *Environmental Research*, 198 (2021).

[38] E. Koubek, Photochemically induced oxidation of refractory organics with hydrogen peroxide, *Industrial & Engineering Chemistry Process Design and Development*, 14 (1975) 348-350.

[39] (!!! INVALID CITATION !!! {}).

[40] B. Xu, N.-Y. Gao, X.-F. Sun, S.-J. Xia, M. Rui, M.-O. Simonnot, C. Causserand, J.-F. Zhao, Photochemical degradation of diethyl phthalate with UV/H<sub>2</sub>O<sub>2</sub>, *Journal of hazardous materials*, 139 (2007) 132-139.

[41] Y. Lv, Y. Liu, J. Wei, M. Li, D. Xu, B. Lai, Bisphenol S degradation by visible light assisted peroxymonosulfate process based on BiOI/B<sub>4</sub>C photocatalysts with Z-scheme heterojunction, *CHEMICAL ENGINEERING JOURNAL*, 417 (2021).

[42] R.R. Solis, F.J. Rivas, O. Gimeno, J.L. Perez-Bote, Synergism between peroxymonosulfate and LaCoO<sub>3</sub>-TiO<sub>2</sub> photocatalysis for oxidation of herbicides. Operational variables and catalyst characterization assessment, *Journal of Chemical Technology and Biotechnology*, 92 (2017) 2159-2170.

[43] J.L. Jia, D.M. Liu, S.X. Wang, H.R. Li, J.X. Ni, X.B. Li, J.Y. Tian, Q. Wang, Visible-light-induced activation of peroxymonosulfate by TiO<sub>2</sub> nano-tubes arrays for enhanced degradation of bisphenol A, *Separation and Purification Technology*, 253 (2020).

[44] W. Zhou, H. Fu, Mesoporous TiO<sub>2</sub>: preparation, doping, and as a composite for

photocatalysis, *ChemCatChem*, 5 (2013) 885-894.

[45] J. Di, M.Z. Zhu, R. Jamakanga, X.K. Gai, Y. Li, R.Q. Yang, Electrochemical activation combined with advanced oxidation on NiCo<sub>2</sub>O<sub>4</sub> nanoarray electrode for decomposition of Rhodamine B, *Journal of Water Process Engineering*, 37 (2020).

[46] H.R. Song, L.X. Yan, J. Jiang, J. Ma, Z.X. Zhang, J.M. Zhang, P.X. Liu, T. Yang, Electrochemical activation of persulfates at BDD anode: Radical or nonradical oxidation?, *Water Research*, 128 (2018) 393-401.

[47] J. Li, Y.J. Li, Z.K. Xiong, G. Yao, B. Lai, The electrochemical advanced oxidation processes coupling of oxidants for organic pollutants degradation: A mini-review, *Chinese Chemical Letters*, 30 (2019) 2139-2146.

[48] I. Firdaus, A. Yaqub, H. Ajab, I. Khan, B.A.Z. Amin, A. Bai, M.H. Isa, Electrochemical oxidation of amoxicillin, ciprofloxacin and erythromycin in water: Effect of experimental factors on COD removal, *Pakistan Journal of Pharmaceutical Sciences*, 34 (2021) 119-128.

[49] J. Teng, G. Liu, J. Liang, S. You, Electrochemical oxidation of sulfadiazine with titanium suboxide mesh anode, *Electrochimica Acta*, 331 (2020).

[50] S. Hammami, N. Bellakhal, N. Oturan, M.A. Oturan, M. Dachraoui, Degradation of Acid Orange 7 by electrochemically generated •OH radicals in acidic aqueous medium using a boron-doped diamond or platinum anode: A mechanistic study, *Chemosphere*, 73 (2008) 678-684.

[51] S. Hammami, M.A. Oturan, N. Oturan, N. Bellakhal, M. Dachraoui, Comparative mineralization of textile dye indigo by photo-Fenton process and anodic oxidation using boron-doped diamond anode, *Desalination and Water Treatment*, 45

(2012) 297-304.

[52] K. Radha, V. Sridevi, K. Kalaivani, Electrochemical oxidation for the treatment of textile industry wastewater, *Bioresource Technology*, 100 (2009) 987-990.

[53] E.A. Agudelo, S.A. Cardona G, Advanced Oxidation Technology (Ozone-catalyzed by Powder Activated Carbon-Portland Cement) for the Degradation of the Meropenem Antibiotic, *Ozone-Science & Engineering*, 43 (2021) 88-105.

[54] Y. Cao, W. Qiu, Y.M. Zhao, J. Li, J. Jiang, Y. Yang, S.Y. Pang, G.Q. Liu, The degradation of chloramphenicol by O-3/PMS and the impact of O-3-based AOPs pre-oxidation on dichloroacetamide generation in post-chlorination, *Chemical Engineering Journal*, 401 (2020).

[55] C.A. Somensi, E.L. Simionatto, S.L. Bertoli, A. Wisniewski Jr, C.M. Radetski, Use of ozone in a pilot-scale plant for textile wastewater pre-treatment: physico-chemical efficiency, degradation by-products identification and environmental toxicity of treated wastewater, *Journal of Hazardous Materials*, 175 (2010) 235-240.

[56] T. Olmez-Hanci, I. Arslan-Alaton, Comparison of sulfate and hydroxyl radical based advanced oxidation of phenol, *Chemical Engineering Journal*, 224 (2013) 10-16.

[57] Z. Han, Z. Li, Y. Li, D. Shang, L. Xie, Y. Lv, S. Zhan, W. Hu, Enhanced electron transfer and hydrogen peroxide activation capacity with N, P-codoped carbon encapsulated CeO<sub>2</sub> in heterogeneous electro-Fenton process, *Chemosphere*, 287 (2022).

[58] N. Javid, Z. Honarmandrad, M. Malakootian, Ciprofloxacin removal from

aqueous solutions by ozonation with calcium peroxide, *Desalination and Water Treatment*, 174 (2020) 178-185.

[59] Z. Honarmandrad, N. Javid, M. Malakootian, Efficiency of ozonation process with calcium peroxide in removing heavy metals (Pb, Cu, Zn, Ni, Cd) from aqueous solutions, *Sn Applied Sciences*, 2 (2020).

[60] L. Xiang, Z. Xie, H. Guo, J. Song, D. Li, Y. Wang, S. Pan, S. Lin, Z. Li, J. Han, W. Qiao, Efficient removal of emerging contaminant sulfamethoxazole in water by ozone coupled with calcium peroxide: Mechanism and toxicity assessment, *Chemosphere*, 283 (2021).

[61] D. Hanh, B. Rajbhandari, A. Annachhatre, Bioremediation of sediments from intensive aquaculture shrimp farms by using calcium peroxide as slow oxygen release agent, *Environmental technology*, 26 (2005) 581-590.

[62] S. Yoshinaga, Direct-seeding cultivation of rice in Japan: stabilization of seedling establishment and improvement of lodging resistance, Copyright International Rice Research Institute 2005, (2005) 184.

[63] K. Zhou, B. Wu, L. Su, X. Gao, X. Chai, X. Dai, Development of nano-CaO<sub>2</sub>-coated clinoptilolite for enhanced phosphorus adsorption and simultaneous removal of COD and nitrogen from sewage, *Chemical Engineering Journal*, 328 (2017) 35-43.

[64] A. Northup, D. Cassidy, Calcium peroxide (CaO<sub>2</sub>) for use in modified Fenton chemistry, *Journal of Hazardous Materials*, 152 (2008) 1164-1170.

[65] A. Goi, M. Trapido, Chlorophenols contaminated soil remediation by peroxidation, *Journal of Advanced Oxidation Technologies*, 13 (2010) 50-58.

- [66] M. Arienzo, Degradation of 2, 4, 6-trinitrotoluene in water and soil slurry utilizing a calcium peroxide compound, *Chemosphere*, 40 (2000) 331-337.
- [67] J. Kozak, M. Włodarczyk-Makuła, Comparison of the PAHs degradation effectiveness using CaO<sub>2</sub> or H<sub>2</sub>O<sub>2</sub> under the photo-Fenton reaction, *Desalination and Water Treatment*, 134 (2018) 57-64.
- [68] Y. Sun, M. Danish, M. Ali, A. Shan, M. Li, Y. Lyu, Z. Qiu, Q. Sui, X. Zang, S. Lyu, Trichloroethene degradation by nanoscale CaO<sub>2</sub> activated with Fe (II)/FeS: The role of FeS and the synergistic activation mechanism of Fe (II)/FeS, *Chemical Engineering Journal*, 394 (2020) 124830.
- [69] X. Zhou, H. Wu, L. Zhang, B. Liang, X. Sun, J. Chen, Activation of Peracetic Acid with Lanthanum Cobaltite Perovskite for Sulfamethoxazole Degradation under a Neutral pH: The Contribution of Organic Radicals, *Molecules*, 25 (2020).
- [70] C. Pironti, F. Dell'Annunziata, R. Giugliano, V. Folliero, M. Galdiero, M. Ricciardi, O. Motta, A. Proto, G. Franci, Comparative analysis of peracetic acid (PAA) and permaleic acid (PMA) in disinfection processes, *Science of the Total Environment*, 797 (2021).
- [71] S. Wang, H. Wang, Y. Liu, Y. Fu, Effective degradation of sulfamethoxazole with Fe<sup>2+</sup>-zeolite/peracetic acid, *Separation and Purification Technology*, 233 (2020).
- [72] R.K. Chhetri, A. Baun, H.R. Andersen, Acute toxicity and risk evaluation of the CSO disinfectants performic acid, peracetic acid, chlorine dioxide and their by-products hydrogen peroxide and chlorite, *Science of The Total Environment*, 677 (2019) 1-8.
- [73] R.K. Chhetri, A. Bonnerup, H.R. Andersen, Combined Sewer Overflow

pretreatment with chemical coagulation and a particle settler for improved peracetic acid disinfection, *Journal of Industrial and Engineering Chemistry*, 37 (2016) 372-379.

[74] A. Eramo, W.R.M. Medina, N.L. Fahrenfeld, Peracetic acid disinfection kinetics for combined sewer overflows: indicator organisms, antibiotic resistance genes, and microbial community, *Environmental science: water research & technology*, 3 (2017) 1061-1072.

[75] Y. Minamitsuji, D. Kato, H. Fujioka, T. Dohi, Y. Kita, Organoiodine-catalyzed oxidative spirocyclization of phenols using peracetic acid as a green and economic terminal oxidant, *Australian journal of chemistry*, 62 (2009) 648-652.

[76] K. Zhang, X. Zhou, P. Du, T. Zhang, M. Cai, P. Sun, C.-H. Huang, Oxidation of  $\beta$ -lactam antibiotics by peracetic acid: Reaction kinetics, product and pathway evaluation, *Water research*, 123 (2017) 153-161.

[77] L. Rizzo, T. Agovino, S. Nahim-Granados, M. Castro-Alf erez, P. Fern andez-Ib a nez, M.I. Polo-L opez, Tertiary treatment of urban wastewater by solar and UV-C driven advanced oxidation with peracetic acid: Effect on contaminants of emerging concern and antibiotic resistance, *Water research*, 149 (2019) 272-281.

[78] L. Rizzo, G. Lofrano, C. Gago, T. Bredneva, P. Iannece, M. Pazos, N. Krasnogorskaya, M. Carotenuto, Antibiotic contaminated water treated by photo driven advanced oxidation processes: Ultraviolet/H<sub>2</sub>O<sub>2</sub> vs ultraviolet/peracetic acid, *Journal of cleaner production*, 205 (2018) 67-75.

[79] Y. Peng, H. Tang, B. Yao, X. Gao, X. Yang, Y. Zhou, Activation of peroxymonosulfate (PMS) by spinel ferrite and their composites in degradation of

organic pollutants: A Review, *Chemical Engineering Journal*, 414 (2021) 128800.

[80] J. Luo, Y. Gao, T. Song, Y. Chen, Activation of peroxymonosulfate by biochar and biochar-based materials for degrading refractory organics in water: A review, *WATER SCIENCE AND TECHNOLOGY*, 83 (2021) 2327-2344.

[81] E.B. Lashkaryani, B. Kakavandi, R.R. Kalantary, A.J. Jafari, M. Gholami, Activation of peroxymonosulfate into amoxicillin degradation using cobalt ferrite nanoparticles anchored on graphene (CoFe<sub>2</sub>O<sub>4</sub>@Gr), *TOXIN REVIEWS*, 40 (2021) 215-224.

[82] J.L. Wang, S.Z. Wang, Activation of persulfate (PS) and peroxymonosulfate (PMS) and application for the degradation of emerging contaminants, *Chemical Engineering Journal*, 334 (2018) 1502-1517.

[83] N. Hashimoto, A. Kanda, Practical and environmentally friendly epoxidation of olefins using oxone, *Organic process research & development*, 6 (2002) 405-406.

[84] G. Cravotto, D. Garella, D. Carnaroglio, E.C. Gaudino, O. Rosati, Solvent-free chemoselective oxidation of thioethers and thiophenes by mechanical milling, *Chemical Communications*, 48 (2012) 11632-11634.

[85] K.N. Parida, S. Jhulki, S. Mandal, J.N. Moorthy, Oxidation of benzyl alcohols, benzyl halides, and alkylbenzenes with oxone, *Tetrahedron*, 68 (2012) 9763-9768.

[86] S. Yan, L. Wei, Y. Duan, H. Li, Y. Liao, Q. Lv, F. Zhu, Z. Wang, W. Lu, P. Yin, Short-term effects of meteorological factors and air pollutants on hand, foot and mouth disease among children in Shenzhen, China, 2009–2017, *International journal of environmental research and public health*, 16 (2019) 3639.

[87] L. Høj, D.G. Bourne, M.R. Hall, Localization, abundance and community

structure of bacteria associated with *Artemia*: Effects of nauplii enrichment and antimicrobial treatment, *Aquaculture*, 293 (2009) 278-285.

[88] T.-J. Kim, Prevention of avian influenza virus by ultraviolet radiation and prediction of outbreak by satellite parameters, *Journal of Biomedical Science and Engineering*, 11 (2018) 182.

[89] T. Kotani, Y. Shiraishi, Y. Tsukamoto, M. Kuwamura, J. Yamate, S. Sakuma, M. Gohda, Epithelial cell kinetics in the inflammatory process of chicken trachea infected with infectious bronchitis virus, *Journal of Veterinary Medical Science*, 62 (2000) 129-134.

[90] F. Tian, J. Luo, H. Zhang, S. Chang, J. Song, MiRNA expression signatures induced by Marek's disease virus infection in chickens, *Genomics*, 99 (2012) 152-159.

[91] S. Eor, J. Hwang, M.G. Choi, S.-K. Chang, Fluorescent signaling of oxone by desulfurization of thioamide, *Organic letters*, 13 (2011) 370-373.

[92] N. Bhatt, Applications of Oxone in chemical kinetics, synthetic chemistry and environmental chemistry: A review, *Environment Conservation Journal*, 18 (2017) 135-140.

[93] J.L. Minor, R.H. Atalla, Strength loss in recycled fibers and methods of restoration, *MRS Online Proceedings Library (OPL)*, 266 (1992).

[94] C. Zhao, B. Shao, M. Yan, Z. Liu, Q. Liang, Q. He, T. Wu, Y. Liu, Y. Pan, J. Huang, J. Wang, J. Liang, L. Tang, Activation of peroxymonosulfate by biochar-based catalysts and applications in the degradation of organic contaminants: A review, *CHEMICAL ENGINEERING JOURNAL*, 416 (2021).

- [95] F. Ghanbari, M. Moradi, Application of peroxymonosulfate and its activation methods for degradation of environmental organic pollutants: Review, *Chemical Engineering Journal*, 310 (2017) 41-62.
- [96] S. Waclawek, H.V. Lutze, K. Grubel, V.V.T. Padil, M. Cernik, D.D. Dionysiou, Chemistry of persulfates in water and wastewater treatment: A review, *Chemical Engineering Journal*, 330 (2017) 44-62.
- [97] S. Yang, P. Wang, X. Yang, L. Shan, W. Zhang, X. Shao, R. Niu, Degradation efficiencies of azo dye Acid Orange 7 by the interaction of heat, UV and anions with common oxidants: Persulfate, peroxymonosulfate and hydrogen peroxide, *Journal of Hazardous Materials*, 179 (2010) 552-558.
- [98] M.G. Antoniou, I. Boraie, M. Solakidou, Y. Deligiannakis, M. Abhishek, L.A. Lawton, C. Edwards, Enhancing photocatalytic degradation of the cyanotoxin microcystin-LR with the addition of sulfate-radical generating oxidants, *Journal of Hazardous Materials*, 360 (2018) 461-470.
- [99] J. Deng, C. Ya, Y.J. Ge, Y.Q. Cheng, Y.J. Chen, M.Y. Xu, H.Y. Wang, Activation of peroxymonosulfate by metal (Fe, Mn, Cu and Ni) doping ordered mesoporous Co<sub>3</sub>O<sub>4</sub> for the degradation of enrofloxacin, *Rsc Advances*, 8 (2018) 2338-2349.
- [100] H. Song, R. Du, Y. Wang, D. Zu, R. Zhou, Y. Cai, F. Wang, Z. Li, Y. Shen, C. Li, Anchoring single atom cobalt on two-dimensional MXene for activation of peroxymonosulfate, *Applied Catalysis B: Environmental*, 286 (2021) 119898.
- [101] L. Wu, Y. Lin, Y. Zhang, P. Wang, M. Ding, M. Nie, C. Yan, S. Chen, Ca(OH)<sub>2</sub>-mediated activation of peroxymonosulfate for the degradation of bisphenol S, *RSC ADVANCES*, 11 (2021) 33626-33636.

[102] J. Miao, W. Geng, P.J.J. Alvarez, M.C. Long, 2D N-Doped Porous Carbon Derived from Polydopamine-Coated Graphitic Carbon Nitride for Efficient Nonradical Activation of Peroxymonosulfate, *Environmental Science & Technology*, 54 (2020) 8473-8481.

[103] Y. Wang, X. Liu, L. Zhang, Assembling 3D hierarchical hollow flower-like Ni@N-doped graphitic carbon for boosting simultaneously efficient removal and sensitive monitoring of multiple sulfonamides, *Journal of Hazardous Materials*, 386 (2020).

[104] Z. Li, Y.Q. Sun, Y. Yang, Y.T. Han, T.S. Wang, J.W. Chen, D.C.W. Tsang, Biochar-supported nanoscale zero-valent iron as an efficient catalyst for organic degradation in groundwater, *Journal of Hazardous Materials*, 383 (2020).

[105] M. Zhu, L. Kong, M. Xie, W. Lu, H. Liu, N. Li, Z. Feng, J. Zhan, Carbon aerogel from forestry biomass as a peroxymonosulfate activator for organic contaminants degradation, *Journal of Hazardous Materials*, (2021) 125438.

[106] Y. Feng, J. Zhong, L.Y. Zhang, Y. Fan, Z.Q. Yang, K.M. Shih, H.L. Li, D.L. Wu, B. Yan, Activation of peroxymonosulfate by Fe-0@Fe<sub>3</sub>O<sub>4</sub> core-shell nanowires for sulfate radical generation: Electron transfer and transformation products, *Separation and Purification Technology*, 247 (2020).

[107] R.B. Li, J.S. Huang, M.X. Cai, J.X. Huang, Z.J. Xie, Q.X. Zhang, Y. Liu, H.J. Liu, W.Y. Lv, G.G. Liu, Activation of peroxymonosulfate by Fe doped g-C<sub>3</sub>N<sub>4</sub>/graphene under visible light irradiation for Trimethoprim degradation, *Journal of Hazardous Materials*, 384 (2020).

[108] A.A.P. Khan, A. Khan, A.M. Asiri, M.A. Rub, Catalyst usage of micro

concentration of Mn(II) for the oxidation of biotin by peroxomonosulphate in aqueous medium: A mechanistic approach, *Journal of Industrial and Engineering Chemistry*, 20 (2014) 3590-3595.

[109] P. Ye, D.M. Wu, M.Y. Wang, Y. Wei, A.H. Xu, X.X. Li, Coating magnetic CuFe<sub>2</sub>O<sub>4</sub> nanoparticles with OMS-2 for enhanced degradation of organic pollutants via peroxymonosulfate activation, *Applied Surface Science*, 428 (2018) 131-139.

[110] J. Xie, Y. Wei, X. Song, Y. Chen, Q. Zou, M. Wang, A. Xu, X. Li, Controlled growth of  $\gamma$ -MnO<sub>2</sub> nanoflakes on OMS-2 for efficient decomposition of organic dyes in aqueous solution via peroxymonosulfate activation, *Journal of Colloid and Interface Science*, 529 (2018) 476-485.

[111] Z.D. Li, D.F. Liu, W.L. Huang, X.C. Wei, W.W. Huang, Biochar supported CuO composites used as an efficient peroxymonosulfate activator for highly saline organic wastewater treatment, *Science of the Total Environment*, 721 (2020).

[112] Z.Q. Chen, L.Y. Wang, H.D. Xu, Q.X. Wen, Efficient heterogeneous activation of peroxymonosulfate by modified CuFe<sub>2</sub>O<sub>4</sub> for degradation of tetrabromobisphenol A, *Chemical Engineering Journal*, 389 (2020).

[113] Z.L. Wang, Y.C. Du, Y.L. Liu, B.H. Zou, J.Y. Xiao, J. Ma, Degradation of organic pollutants by NiFe<sub>2</sub>O<sub>4</sub>/peroxymonosulfate: efficiency, influential factors and catalytic mechanism, *Rsc Advances*, 6 (2016) 11040-11048.

[114] R. Ramachandran, S. Thangavel, L. Minzhang, S. Haiquan, X. Zong-Xiang, F. Wang, Efficient degradation of organic dye using Ni-MOF derived NiCo-LDH as peroxymonosulfate activator, *Chemosphere*, (2020) 128509.

[115] R.X. Yuan, M.L. Jiang, S.M. Gao, Z.H. Wang, H.Y. Wang, G. Boczkaj, Z.J. Liu,

J. Ma, Z.J. Li, 3D mesoporous alpha-Co(OH)<sub>2</sub> nanosheets electrodeposited on nickel foam: A new generation of macroscopic cobalt-based hybrid for peroxymonosulfate activation, *Chemical Engineering Journal*, 380 (2020).

[116] J. Hao, S. Zhao, R. Mao, X. Zhao, Activation of peroxymonosulfate by cobalt doped graphitic carbon nitride for ammonia removal in chloride-containing wastewater, *SEPARATION AND PURIFICATION TECHNOLOGY*, 271 (2021).

[117] B.H. Liu, W.Q. Guo, H.Z. Wang, Q.S. Si, Q. Zhao, H.C. Luo, N.Q. Ren, Activation of peroxymonosulfate by cobalt-impregnated biochar for atrazine degradation: The pivotal roles of persistent free radicals and ecotoxicity assessment, *Journal of Hazardous Materials*, 398 (2020).

[118] Y. Chu, X. Tan, Z. Shen, P. Liu, N. Han, J. Kang, X. Duan, S. Wang, L. Liu, S. Liu, Efficient removal of organic and bacterial pollutants by Ag-La<sub>0.8</sub>Ca<sub>0.2</sub>Fe<sub>0.94</sub>O<sub>3-δ</sub> perovskite via catalytic peroxymonosulfate activation, *Journal of Hazardous Materials*, 356 (2018) 53-60.

[119] M. Qiao, X.F. Wu, S. Zhao, R. Djellabi, X. Zhao, Peroxymonosulfate enhanced photocatalytic decomposition of silver-cyanide complexes using g-C<sub>3</sub>N<sub>4</sub> nanosheets with simultaneous recovery of silver, *Applied Catalysis B-Environmental*, 265 (2020).

[120] B. Bouzayani, E. Rosales, M. Pazos, S.C. Elaoud, M.A. Sanromán, Homogeneous and heterogeneous peroxymonosulfate activation by transition metals for the degradation of industrial leather dye, *Journal of Cleaner Production*, 228 (2019) 222-230.

[121] C. Pan, L. Fu, Y. Ding, X. Peng, Q. Mao, Homogeneous catalytic activation of

peroxymonosulfate and heterogeneous reductive regeneration of  $\text{Co}^{2+}$  by  $\text{MoS}_2$ : The pivotal role of pH, *Science of The Total Environment*, 712 (2020) 136447.

[122] Z. Li, F. Wang, Y. Zhang, Y. Lai, Q. Fang, Y. Duan, Activation of peroxymonosulfate by  $\text{CuFe}_2\text{O}_4$ - $\text{CoFe}_2\text{O}_4$  composite catalyst for efficient bisphenol a degradation: Synthesis, catalytic mechanism and products toxicity assessment, *CHEMICAL ENGINEERING JOURNAL*, 423 (2021).

[123] G.P. Anipsitakis, D.D. Dionysiou, Degradation of Organic Contaminants in Water with Sulfate Radicals Generated by the Conjunction of Peroxymonosulfate with Cobalt, *Environmental Science & Technology*, 37 (2003) 4790-4797.

[124] P. Wang, S. Yang, L. Shan, R. Niu, X. Shao, Involvements of chloride ion in decolorization of Acid Orange 7 by activated peroxydisulfate or peroxymonosulfate oxidation, *Journal of environmental sciences*, 23 (2011) 1799-1807.

[125] E.R. Bandala, M.A. Peláez, D.D. Dionysiou, S. Gelover, J. Garcia, D. Macías, Degradation of 2,4-dichlorophenoxyacetic acid (2,4-D) using cobalt-peroxymonosulfate in Fenton-like process, *Journal of Photochemistry and Photobiology A: Chemistry*, 186 (2007) 357-363.

[126] T. Chen, Z. Zhu, Z. Wang, H. Zhang, Y. Qiu, D. Yin, G. Zhao, 3D hollow sphere-like Cu-incorporated  $\text{LaAlO}_3$  perovskites for peroxymonosulfate activation: Coaction of electron transfer and oxygen defect, *Chemical Engineering Journal*, 385 (2020) 123935.

[127] J.B. Chen, L.M. Zhang, T.Y. Huang, W.W. Li, Y. Wang, Z.M. Wang, Decolorization of azo dye by peroxymonosulfate activated by carbon nanotube: Radical versus non-radical mechanism, *Journal of Hazardous Materials*, 320 (2016)

571-580.

[128] C.X. Wang, P.H. Shi, X.D. Cai, Q.J. Xu, X.J. Zhou, X.L. Zhou, D. Yang, J.C. Fan, Y.L. Min, H.H. Ge, W.F. Yao, Synergistic Effect of Co<sub>3</sub>O<sub>4</sub> Nanoparticles and Graphene as Catalysts for Peroxymonosulfate-Based Orange II Degradation with High Oxidant Utilization Efficiency, *Journal of Physical Chemistry C*, 120 (2016) 336-344.

[129] Y. Sun, D. Li, S. Zhou, K.J. Shah, X. Xiao, Research Progress of Advanced Oxidation Water Treatment Technology, *Advances in Wastewater Treatment II*, 102 (2021) 1-47.

[130] R. Matta, S. Tlili, S. Chiron, S. Barbati, Removal of carbamazepine from urban wastewater by sulfate radical oxidation, *Environmental chemistry letters*, 9 (2011) 347-353.

[131] S.-H. Do, J.-H. Jo, Y.-H. Jo, H.-K. Lee, S.-H. Kong, Application of a peroxymonosulfate/cobalt (PMS/Co(II)) system to treat diesel-contaminated soil, *Chemosphere*, 77 (2009) 1127-1131.

[132] W. Han, L. Dong, Activation Methods of Advanced Oxidation Processes Based on Sulfate Radical and Their Applications in The Degradation of Organic Pollutants, *PROGRESS IN CHEMISTRY*, 33 (2021) 1426-1439.

[133] J. Wang, S. Wang, Activation of persulfate (PS) and peroxymonosulfate (PMS) and application for the degradation of emerging contaminants, *Chemical Engineering Journal*, 334 (2018) 1502-1517.

[134] Y. Fan, Y.F. Ji, G.Y. Zheng, J.H. Lu, D.Y. Kong, X.M. Yin, Q.S. Zhou, Degradation of atrazine in heterogeneous Co<sub>3</sub>O<sub>4</sub> activated peroxymonosulfate

oxidation process: Kinetics, mechanisms, and reaction pathways, *Chemical Engineering Journal*, 330 (2017) 831-839.

[135] P.R. Shukla, S.B. Wang, H.Q. Sun, H.M. Ang, M. Tade, Activated carbon supported cobalt catalysts for advanced oxidation of organic contaminants in aqueous solution, *Applied Catalysis B-Environmental*, 100 (2010) 529-534.

[136] Y. Zhang, W. Chu, Cooperation of multi-walled carbon nanotubes and cobalt doped TiO<sub>2</sub> to activate peroxymonosulfate for antipyrine photocatalytic degradation, *Separation and Purification Technology*, (2021) 119996.

[137] J. Zhang, M.Y. Chen, L. Zhu, Activation of persulfate by Co<sub>3</sub>O<sub>4</sub> nanoparticles for orange G degradation, *Rsc Advances*, 6 (2016) 758-768.

[138] Q. Liu, Q. Wang, W. Deng, L. Gong, T. Sun, C. Liu, X. Huang, G. Liu, Z. Huang, Templated Solid-State Fabrication of Quadrangled Mn–Co Mesoporous Oxides for Degradation of Methylene Blue in Water, *Environmental Engineering Science*, 36 (2019) 1199-1205.

[139] Q. Wang, Y. Shao, N. Gao, W. Chu, J. Chen, X. Lu, Y. Zhu, N. An, Activation of peroxymonosulfate by Al<sub>2</sub>O<sub>3</sub>-based CoFe<sub>2</sub>O<sub>4</sub> for the degradation of sulfachloropyridazine sodium: Kinetics and mechanism, *Separation and Purification Technology*, 189 (2017) 176-185.

[140] M.-P. Zhu, J.-C.E. Yang, X. Duan, S. Wang, D.S. Delai, B. Yuan, M.-L. Fu, Engineered Co<sub>2</sub>AlO<sub>4</sub>/CoAl<sub>2</sub>O<sub>4</sub>@Al<sub>2</sub>O<sub>3</sub> monolithic catalysts for peroxymonosulfate activation: Co<sup>3+</sup>/Co<sup>2+</sup> and O-Defect/O-Lattice ratios dependence and mechanism, *CHEMICAL ENGINEERING JOURNAL*, 409 (2021).

[141] S. Zhu, Y. Xu, Z. Zhu, Z. Liu, W. Wang, Activation of peroxymonosulfate by

magnetic Co-Fe/SiO<sub>2</sub> layered catalyst derived from iron sludge for ciprofloxacin degradation, *Chemical Engineering Journal*, 384 (2020) 123298.

[142] Q.N. Meng, K. Wang, Y.F. Tang, K. Zhao, G.J. Zhang, Z.H. Han, J. Yang, Facile Synthesis of Porous Flower-Like Co<sub>3</sub>O<sub>4</sub>-SiO<sub>2</sub> Composite for Catalytic Decoloration of Rhodamine B, *Chemistryselect*, 2 (2017) 10442-10448.

[143] S. Krishna, P. Sathishkumar, N. Pugazhenthiran, K. Guesh, R.V. Mangalaraja, S. Kumaran, M.A. Gracia-Pinilla, S. Anandan, Heterogeneous sonocatalytic activation of peroxomonosulphate in the presence of CoFe<sub>2</sub>O<sub>4</sub>/TiO<sub>2</sub> nanocatalysts for the degradation of Acid Blue 113 in an aqueous environment, *Journal of Environmental Chemical Engineering*, 8 (2020).

[144] I.A. Slavova, S.G. Christoskova, M.K. Stoyanova, Catalytic oxidation of Rhodamine B in aqueous solutions with sulphate radicals over Co<sub>3</sub>O<sub>4</sub>/MgO and CoFe<sub>2</sub>O<sub>4</sub>/MgO, *Bulgarian Chemical Communications*, 49 (2017) 761-767.

[145] J.K. Du, J.G. Bao, Y. Liu, H.B. Ling, H. Zheng, S.H. Kim, D.D. Dionysiou, Efficient activation of peroxymonosulfate by magnetic Mn-MGO for degradation of bisphenol A, *Journal of Hazardous Materials*, 320 (2016) 150-159.

[146] X. Fu, J. Zhang, H. Zhao, S. Zhang, T. Nie, Y. Zhang, J. Lu, Enhanced peroxymonosulfate activation by coupling zeolite-supported nano-zero-valent iron with weak magnetic field, *Separation and Purification Technology*, 230 (2020) 115886.

[147] H. Chen, Y. Yang, J. Wei, J. Xu, J. Li, P. Wang, J. Xu, Y. Han, H. Jin, D. Jin, X. Peng, B. Hong, H. Ge, X. Wang, Cobalt ferrites/activated carbon: Synthesis, magnetic separation and catalysis for potassium hydrogen persulfate, *Materials*

Science and Engineering: B, 249 (2019) 114420.

[148] S. Chen, X.D. Liu, S.Y. Gao, Y.C. Chen, L.J. Rao, Y.Y. Yao, Z.W. Wu, CuCo<sub>2</sub>O<sub>4</sub> supported on activated carbon as a novel heterogeneous catalyst with enhanced peroxymonosulfate activity for efficient removal of organic pollutants, *Environmental Research*, 183 (2020).

[149] S.Y. Yang, T. Xiao, J. Zhang, Y.Y. Chen, L. Li, Activated carbon fiber as heterogeneous catalyst of peroxymonosulfate activation for efficient degradation of Acid Orange 7 in aqueous solution, *Separation and Purification Technology*, 143 (2015) 19-26.

[150] L. Hu, X. Yang, S. Dang, An easily recyclable Co/SBA-15 catalyst: Heterogeneous activation of peroxymonosulfate for the degradation of phenol in water, *Applied Catalysis B: Environmental*, 102 (2011) 19-26.

[151] R.X. Yuan, L. Hu, P. Yu, Z.H. Wang, H.Y. Wang, J.Y. Fang, Co<sub>3</sub>O<sub>4</sub> nanocrystals/3D nitrogen-doped graphene aerogel: A synergistic hybrid for peroxymonosulfate activation toward the degradation of organic pollutants, *Chemosphere*, 210 (2018) 877-888.

[152] Y. Zhang, J.-B. Huo, J.-C.E. Yang, M.-L. Fu, Facile fabrication of elastic CoO@graphene aerogel for recycled degradation of chloramphenicol, *Materials Letters*, 240 (2019) 88-91.

[153] L. Peng, X.B. Gong, X.H. Wang, Z. Yang, Y. Liu, In situ growth of ZIF-67 on a nickel foam as a three-dimensional heterogeneous catalyst for peroxymonosulfate activation, *Rsc Advances*, 8 (2018) 26377-26382.

[154] R.X. Yuan, L. Hu, P. Yu, H.Y. Wang, Z.H. Wang, J.Y. Fang, Nanostructured

Co<sub>3</sub>O<sub>4</sub> grown on nickel foam: An efficient and readily recyclable 3D catalyst for heterogeneous peroxymonosulfate activation, *Chemosphere*, 198 (2018) 204-215.